DESIGN OF A MAGNETIC MEASUREMENT SYSTEM FOR SMALL SATELLITES

MASTER THESIS

MAY 24, 2023

Author:
D.H.T. van den Beld (5172993/1001770)

Supervisors:
dr. ir. Jasper Bouwmeester
prof. dr. Roger Jaspers

Delft University of Technology

Design of a Magnetic Measurement System for Small Satellites

Towards the Optimization of ADCS Magnetometer Performance

by

D.H.T. van den Beld

to obtain the degree of Master of Science
at the Delft University of Technology,
to be defended publicly on 07-06-2023
in lecture room F of the Aerospace Engineering faculty.

Student Number:	5172993		
Project Duration:	Feb, 2022 - May, 2023		
Thesis Committee:	dr. J. Guo,	TU Delft,	SSE (Head of Committee)
	dr. ir. J. Bouwmeester,	TU Delft,	SSE (Supervisor)
	dr. ir. W. van der Wal,	TU Delft,	AS
	dr. S. Speratta,	TU Delft,	SSE
Faculty:	Faculty of Aerospace Engineering, Delft		

An electronic version of this thesis is available at http://repository.tudelft.nl/.

TU Delft

Abstract

ADCS magnetometers on board of satellites suffer from the disruptive magnetic field produced by the satellite itself. For CubeSats and PocketQubes this magnetic field is usually not quantified. If the largest magnetic field sources are known and if there is freedom in the magnetometer placement, the magnetometer is simply placed as far from the largest sources as possible. The magnetometer is not calibrated for the remaining error due to the satellite magnetic field.
The research objective of this thesis is, 'to develop a measurement system which is capable of characterizing the satellite magnetic fields of CubeSats and PocketQubes close to the satellite body itself'. The measurement system is specifically designed for PocketQubes and is designed using the steps of the engineering design process. The design and manufacturing process was conducted separately for three subsystems; the magnetometers, the supporting structure and the data acquisition and processing. The measurement system features four magnetometers, which can be placed in various locations around the satellite with an accuracy of 0.6 mm. In the functional validation several magnetometer configurations were tested using the Delfi-PQ PocketQube as a test case. The functional validation showed that the magnetometers measure the magnetic field produced by a PocketQube with an uncertainty of 0.2 µT for each axis. The magnetic field of the test case, Delfi-PQ, ranges from approximately 5 µT close to the battery pack to 0.5 µT close to the bottom of the satellite. The measurement system can detect dynamic components of the field up to a limiting frequency of 18 Hz, this can in turn be used to trace magnetic noise contributions back to their source.
The uncertainty of 0.2 µT for each axis allows for calibration of on board ADCS magnetometers up to this uncertainty. For an ADCS magnetometer placed at the bottom of Delfi-PQ, this means a reduction in measurement uncertainty from 0.5 µT to 0.2 µT. This reduction would reduce the pointing error introduced by the satellite magnetic field disturbance *and* EMF model uncertainty from 0.6 to 0.3 degrees for the magnetic inclination and 1.5 to 0.7 degrees for the magnetic declination. The measurement system can also be used to select the optimal location for placing ADCS magnetometers, based on where the satellite magnetic field is the lowest and least dynamic.
The measurement system is not designed to conduct measurements on Delfi-PQ with the antennae deployed, this is a missed input requirement and a recommendation for future work. Additionally, the calibration of the magnetometers features a residual linearity error, the reduction of which is recommended as the subject of future work.

Acknowledgements

I would like to take a moment to thank a couple of people who made a contribution to the completion of this thesis project. Most importantly, I would like to thank my supervisors, Jasper Bouwmeester and Roger Jaspers. I would like to express my deepest appreciation to Jasper Bouwmeester for his guidance during our many meetings and his invaluable advise. I would like to express my gratitude to Roger Jaspers, for his insights over the course of this project.

Next, I would like to thank Yannick de Jong for sharing his expertise. Your help has been worth a lot to me and I have learned a lot from you.

I would like to thank Stefano Speretta and Sevket Uludag for their help and advice with the measurements on Delfi-PQ. Using my measurement system on Delfi-PQ was very satisfying, and I am grateful to you for providing me with this opportunity.

I would like to express my gratitude to Herman de Jong. You helped me with setting up the Helmholtz coil system and gave me advice on how to approach the calibration procedure. Your experimental knowledge and willingness to share this with me has been very valuable to me.

Also, I would like to express my appreciation to Maikel Morren. You shared your expertise on various issues, both physics and mathematics related, and took the time to guide me to understanding.

Lastly I would like to mention that I have greatly enjoyed the time I have spent on this thesis project. I would not have enjoyed this time as much if it weren't for Anne, whom I would like to thank for her support during this project. I also greatly appreciate the support my parents Bernard and Carina, have given me over the course of my entire studies. I would like to thank my sisters, Leonoor and Evelien, and my friends for the same thing.

David van den Beld
Delft, May 2023

Contents

List of Figures

List of Tables

List of Abbreviations

Abbreviation	Description
ADCS	Attitude Determination and Control System
AMR	Anisotropic Magnetoresistance
CDA	Centered Dipole Approximation
DUT	Device Under Testing
ECSS	European Coorperation for Space Standardization
EMC	Electromagnetic Compatibility
EMF	Earth Magnetic Field
EMI	Electromagnetic Interference
ESA	European Space Agency
HC system	Helmholtz Coil system
IC	Integrated Circuit
IGRF model	International Geomagnetic Reference Field model
LEO	Low Earth Orbit
LSB	Least Significant Bit
M	Magnetometer (followed by a number)
MCE	Magnetically Clean Environment
MEMS	Microelectromechanical Systems
MI	Magneto Inductive
MR	Magneto Resistive
PLA	Polylactic Acid
PSD	Power Spectral Density
S/C	Spacecraft
SV	Secular Variation
WMM	World Magnetic Model

List of Symbols

Symbol	Description	SI Units
B	Magnetic field	T
H	Magnetic field strength	A/m
B_{DUT}	DUT magnetic field	μT
H_e	Earth magnetic field strength	A/m
μ_0	Vacuum permeability	H/m
c	Speed of light	m/s
J	Current density	A/m^2
ϵ_0	Vacuum permittivity	F/m
μ_0	Vacuum permeability	μNA^{-2}
E	Electric field	V/m
t	Time	s
I	Current	A
h	Height	m
r	Radius or distance	m
a	Radius	m
m	Mass	kg
ω	Frequency	Hz
q	Elementary charge	C
θ	Angle	Degrees
σ	Standard deviation	
σ_m	Standard deviation of the mean	
N	Number of measurements / number of turns	
τ	Period of an oscillation	s

1 Introduction

1.1. Introduction to the problem

Satellites are of tremendous importance for humanity, they play a vital role in internet communications, Earth observation and much more. The recent decade has seen an increase in the deployment of CubeSats [6], with hundreds of them being launched each year [7]. CubeSats are characterized by their standardized design, modularity, light weight and small volume [8]. An important subsystem of any satellite, and thus also of the CubeSat, is the attitude determination and control system. For any active attitude determination and control system, a type of sensor is needed to get knowledge on the CubeSat's orientation. One such sensor is the magnetometer, which provides direct measurements for control using magnetorquers. The magnetometer is known to suffer from larger inaccuracies than, for example, star trackers [9, 10], but comes with the advantage of being cheaply available. For this reason, many CubeSat attitude determination and control systems use a magnetometer [11]. The usage of magnetometers results in a pointing error for the CubeSat, due to the error in on board magnetometer readings. A factor which contributes to the on board magnetometer reading error is the magnetic field the satellite itself produces.

How large the effect of this satellite magnetic field is, is not found in literature. In most CubeSats, the magnetometer is simply placed on the side of the satellite, in an attempt to create as much physical separation between the magnetometer and the rest of the satellite [12]. To improve the pointing accuracy of CubeSats, whilst still using the cheap solution of commercial-off-the-shelf (COTS) magnetometers, more knowledge on the satellite magnetic field is needed.

Currently (April 2023), a lot of information regarding small satellite magnetic fields is unknown. What magnitude the CubeSat field typically has, whether it is dynamic or static, where magnetometers can best be placed on the satellite, are all questions to which literature has no answer. This thesis project aims to address the knowledge gap regarding satellite magnetic fields and to answer these questions. To achieve this, measurements of CubeSat and PocketQube magnetic fields are needed. Knowledge of these fields can be used to improve ADCS performance in CubeSats and PocketQubes. For this purpose, a magnetic field measurement system is built, which can measure the magnetic field at positions close by the surface of a CubeSat or PocketQube.

1.2. Current satellite magnetic field measurements

Magnetometers used for the attitude determination and control system on satellites are exposed to the satellite stray magnetic field close to the satellite body itself. Currently, characterization of CubeSat and PocketQube magnetic fields is not done in literature, and for other (larger) satellites the magnetic field is often only measured far away from the satellite body itself. The following examples illustrate this fact.

The European Coorperation for Space Standardization has a handbook which describes the standards for testing the electromagnetic compatibility (EMC) of a spacecraft [13]. These standards are used by the European space industry, and thus often also by ESA. This handbook (ECSS-E-ST-20-07C) describes, amongst others, the method for testing the DC magnetic field emission and the magnetic moment of the spacecraft. This method relies on the Centered Dipole Approximation (CDA) to model the satellite magnetic field. The CDA requires measurements taken at a distance of >3 times the size of the S/C to allow for a good approximation of the satellite magnetic field[13]. Thus magnetic field structures closer to the satellite might be overlooked

in the CDA. For this reason, the ECSS EMC testing method is not sufficient to characterize the magnetic field close to magnetometers located on the satellite.

The GOCE satellite has been subjected to electromagnetic compatibility testing, outlined in Baklezos et al. (2019) [14]. In this paper the magnetic fields produced by the command and data handling unit (CDMU) were measured using search coil magnetometers in a gradiometer configuration. These measurements were conducted with distances over 0.5 m between the DUT and the search coils.
Similarly, one of the European SWARM satellites has been tested at the German IABG MGSE facility [15]. This facility provides a magnetically clean environment for electromagnetic compatibility testing. For these tests, 6 triaxial fluxgate magnetometers were used, which were once again located mainly in the far field regime. Only at the start of the measurements, 4 of the magnetometers are located closer to the DUT, for the purpose of obtaining a signal to noise ratio. For the purpose of obtaining the actual magnetic field the magnetometers were placed further away again [16].
The above examples illustrate that there is a lack in literature regarding the satellite magnetic field in close proximity to itself.
From this point onward, any mention of 'the satellite magnetic field' will refer to 'the satellite magnetic field within 3 times the satellite body dimension'.

1.3. Research objective

To limit the scope of this thesis project, the choice is made to characterize the magnetic field of small satellites through experimental means, rather than though modelling effort. In this context, the term small satellites encompasses PocketQubes, CubeSats and their subsystems.
The choice to focus on PocketQubes and CubeSats is based on the fact that they have increased greatly in popularity over the last decade [6] and have a standardized design. This makes is feasible to come up with a generalized characterization method which is applicable to a large amount of satellites. Also, due to the strict budget requirements of most CubeSats and PocketQubes, COTS magnetometers are often used in the attitude determination and control system without properly characterizing the satellite magnetic field. Thus, there is a big opportunity regarding the optimization of CubeSat and PocketQube ADCS performance by characterizing the satellite magnetic field.
The choice to take an experimental approach, as opposed to a modelling approach, has a few reasons.
Firstly, a model will always be an approximation of reality at best, and will need measurements for validation. By conducting experiments, the actual satellite magnetic field can be measured, whilst validation can be conducted using a different magnetic field source. Thus an experimental approach enables characterization and validation through experimental means, whereas modelling requires experimental validation.
Secondly, a modelling approach will require extensive knowledge about the satellite architecture. Knowledge about current flows, material properties and even manufacturing methods is needed to produce an accurate model. For many satellites, this knowledge is not available or not well documented, making detailed modelling of the satellite magnetic field laborious.
Based on these decisions, the following research objective has been defined for this thesis project.

To develop a measurement system which is capable of characterizing the satellite magnetic fields of small satellites close to the satellite body itself.

Such a measurement system can be a useful tool for designer teams who desire detailed knowledge about the magnetic field produced by their satellite. Examples being if a magnetically sensitive payload is to be used, or if an optimized attitude determination and control system is desired.

1.4. Research questions

To fulfill the research objective, a magnetic measurement system needs to be created. To do this in a structured manner, and to ensure that the design process does not diverge too much from the research objective, research questions are defined in this section.

The purpose of the magnetic measurement system is stated in the research objective. The first research question addresses how the system will be used and what it needs to be capable of to fulfill the research objective.

1 What applications will a measurement system for small satellites have and what capabilities should such a measurement system have?

The answer to research question 1 will encompass the specification of system requirements, which are in turn used to design and manufacture the measurement system. Once this is accomplished, verification and validation tests need to be conducted. What the system verification and validation tests should look like, is the focus of the second research question.

2 What verification and validation procedures are suitable to test whether the magnetic measurement system fulfills the research objective?

After the system verification and validation it will turn out that the system either fulfills the research objective, or does not do so in its entirety. At this stage it is useful to revisit the topic of what the purpose of the magnetic measurement system is. If the system does pass the validation, additional uses for the system will be explored. If the system does not pass the validation, possible uses which fulfill its original purpose to a certain degree will be explored.

3 What purpose can the designed magnetic measurement system fulfill, either in addition to its original purpose, or instead of its original purpose?

1.5. Methodology

To fulfill the research objective, a magnetic measurement system needs to be created. This thesis project is thus design oriented. The design and manufacturing of this system will be done in several steps, together known as the engineering design process [17]. There are many different formulations of the engineering design process, but most boil down to (atleast) the following steps [17, 18, 19]:

1. Define problem
2. Specify system requirements
3. Preliminary design
4. Detailed design
5. Manufacture
6. Verification and validation.

It should be noted that these steps are part of an iterative process. It is to be expected that one looks back to, and alters, the first steps in the process multiple times whilst already having started later steps. This thesis project will follow these engineering design steps.
Step 1, the problem definition, has been tackled in the introduction. Step 2 focuses on specification of the system requirements. The requirements are separated into four different categories, being

- the system as a whole,
- the magnetometers,
- the supporting structure,
- data acquisition and processing.

The last three categories are the three subsystems of the measurement system. The system requirements, and their verification methods, will be defined in Chapter 2.

Steps 3, 4 and 5 of the engineering design process concern the design and manufacturing of the measurement system. These steps were conducted in parallel for each of the subsystems, and will thus be grouped and discussed per different subsystem. Section 3.1 will discuss the magnetometer selection, which is based on the magnetometer requirements defined before. Section 3.2 will discuss the design of the (supporting) structure of the measurement system. Section 3.3 will discuss the design of the data acquisition and processing subsystem. Chapter 4 will explain the calibration of the magnetometers.

To see whether the measurement system meets the system requirements defined in step 2, a system verification will be conducted. To test whether the measurement system accomplishes the research objective, a functional validation will be conducted. The verification and validation procedures are the focus of research question 2. The result of the system verification and validation will determine whether research question 3 will focus on additional or alternative uses for the measurement system. Both the verification and functional validation are discussed in Chapter 5. Lastly the conclusion is presented in Chapter 6.

2

System Requirements

Step 2 of the engineering design process is to specify the system requirements for the magnetic field measurement system. This also falls within the scope of research question 1, which reads, "What applications will a measurement system for small satellites have and what capabilities should such a measurement system have?".
Before specifying the system requirements, the usage and required accuracy of on board ADCS magnetometers is discussed, in Section 2.1. Following this, the system requirements will be specified in Sections 2.2 to 2.5.

2.1. Accuracy requirements for ADCS magnetometers

Before defining the system requirements, more background on the usage of on board magnetometers is provided. In this section the accuracy an on board magnetometer needs to have is discussed. This is used to define the maximum allowed uncertainty the to be designed measurement system is allowed to have.

When using a magnetometer for attitude determination and/or pointing of the spacecraft, the measured magnetic field is compared to a reference model of the magnetic field [20, 21]. Comparison to this reference field allows for estimation of the spacecraft's current location and pointing angle. Two factors which contribute to the eventual error in the spacecraft's pointing angle (and attitude) in this method are, the error in the measured magnetic field and the error in the reference magnetic field. The error in the measured magnetic field can be influenced by e.g. the magnetometer choice and minimisation of the satellite stray field effects [22, 23]. The error in the reference field, on the other hand, is inherent to the chosen magnetic field model [24]. To determine the allowed error in the measured magnetic field, the error in the reference magnetic field needs to be quantified first. This is done for two different magnetic field models.

2.1.1. International Geomagnetic Reference Field Model

The International Geomagnetic Reference Field model (IGRF) is a model of the Earth magnetic field which is updated every 5 years, from 1900 to 2025. As the model is updated once every 5 years, any single model is made to predict the magnetic field 5 years into the future. Once an updated model is created, the previous model's predictions are evaluated using the actual measured data. It is this evaluation which allows for a predicted uncertainty to be released with every update of the IGRF.
The IGRF takes into account the linear component of secular variation (SV), which is the slow variation of the EMF, but fails to capture the non-linear components of SV such as geomagnetic jerks [21]. When making an IGRF model, lets say in 2020, it is impossible to be certain about the exact nature of SV for the coming 5 years, thus SV is included in the model as a predicted component. The error between the modelled and real magnetic field induced by SV is called a commission error, and it is obvious that this error is not constant in time (it is likely to be bigger as one gets farther from the last update of the IGRF) [24]. For the 2015-2020 IGRF model, the error introduced by secular variation grew from 0 nT to 110 nT. This error is defined as the RMS misfit between the SV models for the 2015-2020 generation IGRF, and the 2020 IGRF model (the next generation, based on new measurement data) [24].

Apart from the error introduced by SV, there are other errors in the IGRF model. As in any model, the IGRF is a simplified depiction of reality, and there are effects which are not included in the model. Errors introduced by such effects are known as omission errors. Omission errors are known to dominate over commission errors [25], and the omission of crustal fields is the most dominant omission error [25, 21]. Crustal fields are not included in the model as they have small-scale variations [21].
The total uncertainty in the IGRF model has been analysed by Beggan et al. (2022) [21], with the purpose to provide users of the IGRF an averaged uncertainty. The results of this study show that the IGRF has a 68.3% confidence interval of 87 nT, 73 nT and 114 nT in the x, y and z directions respectively, with the standard deviations being 144 nT, 136 nT and 293 nT in the x, y and z directions respectively. The difference between the CI intervals and standard deviations finds its root in the fact that the magnetic residuals are distributed according to a Laplacian distribution [21, 26]. These error values are also shown in Table 2.1.

2.1.2. The World Magnetic Model

The World Magnetic Model (WMM) [25] is a very similar model to the previously discussed IGRF. Just like the IGRF, the WMM is constructed using spherical harmonics. As to be expected, both models yield similar results. Yet the error analysis of the WMM includes some aspects which are not included in the error analysis of the IGRF model. In this section focus lies on the 2020-2025 WMM.
Like the IGRF, the WMM includes a commission error. This error is largely caused by SV, but an additional fitting error is also included. This yields a commission error of 46 nT, 53 nT and 84 nT in the x, y and z directions respectively for the year 2025.
The omission error in the WMM has two components, one attributed to crustal fields and one to disturbance fields. Crustal fields are fields generated in the Earth's crust (and not in the core) and disturbance fields are fields generated due to ionospheric, magnetospheric currents and induced currents due to the Earth's oceans. These errors are shown in Table 2.1.
Combining the commission and omission errors of the WMM, a total (RMS) error in the year 2025 of 135 nT, 101 nT and 168 nT in the x, y and z directions respectively.

Row		X (nT)	Y (nT)	Z (nT)
1	IGRF 68.3% CI	87	73	114
2	IGRF standard deviation	144	136	293
3	WMM commission error 2020	3	3	5
4	WMM commission error 2025	46	53	84
5	WMM crustal field error	122	83	143
6	WMM disturbance field error	37	23	27
7	WMM combined 2020	127	86	146
8	WMM combined 2025	135	101	168

Table 2.1: Errors in both the IGRF and WMM magnetic field models. The WMM values are RMS values.

2.1.3. Magnetometer uncertainty

Both the IGRF and WMM models yield similar uncertainties, as can be seen in Table 2.1, but the values do differ slightly. As the WMM has documented the origin of the uncertainties in its model more extensively than the IGRF, the uncertainties presented in row 8 of Table 2.1 will be used as the expected uncertainties present in the reference magnetic field.
The total uncertainty for the ADCS will be the RMS sum of the reference field uncertainty (row 8 in Table 2.1) and the uncertainty in the on board magnetometer measurements. To ensure that the measurements do not increase the total uncertainty too severely, an initial uncertainty requirement of 50% of the reference field uncertainty will be placed on the magnetometer readings.
For any COTS magnetometer the uncertainties in all 3 axes are (almost) similar. For this reason, the average uncertainty of the x, y and z directions in row 8 of Table 2.1 will be used to determine the accuracy requirement for the magnetometer, which yields a total uncertainty of 68 nT. Using this additional uncertainty, the total (RMS) uncertainty, considering both the reference model and measurement uncertainty, can be calculated. The results being an uncertainty of 151 nT, 122 nT and 181 nT in the x, y and z directions respectively. It can clearly be seen that due to the reference model error dominating, the increase in the total error due to

the measurement error is small (20% increase at most). The allowed uncertainty for on board measurements is thus 68 nT.

2.2. Full system requirements

In the next sections the system requirements are presented. Each requirement will be preceded by the reasoning from which the requirement is derived. A verification method follows the requirement if the requirement in question calls for it. The starting number of the requirement indicates whether the requirement relates to, the system as a whole (1), the supporting structure of the system (2), the magnetometers used in the system (3) or the data acquisition and processing subsystem (4).
This section discusses the requirements related to the full measurement system.

2.2.1. Full system functions

The primary goal of the measurement system is to conduct magnetic field measurements on and/or around the DUT (device under testing, in this context either the satellite or an individual subsystem). Measurements inside the DUT will not be considered, as this requires partial disassembly of the DUT or might endanger the DUT. Magnetic measurements will be conducted at several positions around the DUT. This will provide a collection of graphs showing the measured magnetic field as a function of time in the x-, y- and z-directions at the magnetometer positions.

1.1 The system shall be able to measure the magnetic field produced by the DUT at different positions around and/or on the DUT.

1.1.1 The measurement system shall be able to produce a graph of the magnetic field over time on the positions where the field was measured.

A magnetometer measures the total magnetic field produced by everything around it, including the magnetic field that might be produced by the measurement system itself. As this adds an error to the measured DUT magnetic field, the magnetic field produced by the measurement system needs to be as small as possible. This will mean that no magnetic materials can be used in the measurement system. The magnetometers themselves will produce a small magnetic field, as there are currents running through them, and they will therefore also interfere with the readings from one another. As shielding between the magnetometers will disrupt the magnetic field, the interference caused by one magnetometer on another is unavoidable. Yet it needs to be quantified, and a 'safe' distance between the magnetometers needs to be established (addressed in requirement 3.2).

1.2 No magnetic materials shall be used in the supporting structure of the measurement system.

To verify this requirement, an analysis of the used materials will be conducted.
Next to the magnetic field produced by the measurement system itself, the background magnetic field will also disturb the measurements from the system. Whereas a constant magnetic field can easily be accounted for using a calibration measurement, any time-varying magnetic fields will affect the measurement results. In order to get rid of these disturbances, the measurement system shall be placed in a magnetically clean environment (MCE) when it is used to obtain measurement results.

1.3 The measurement system shall be used in a magnetically clean environment.

This requirement will be verified by conducting a measurement in the MCE without a DUT present. If this measurement returns the (constant) EMF, the requirement is considered fulfilled.

2.2.2. System cost

To define the budget for this measurement system, the added value of the measurement system needs to be analysed. The system will be primarily used by the PocketQube team of the TU Delft. At the moment the PocketQube team is capable of designing and building PocketQubes which obtain mission success without using a magnetic measurement system. For future mission, it is desired to increase the ADCS performance

of the satellite, for which knowledge of the magnetic field of the satellite itself is essential. Currently a single estimate is used to determine the satellite magnetic field. This estimate does not take into account the different operational modes of the satellite. Using a magnetic measurement system, the satellite magnetic field can be determined for different operational modes, and thus the performance of the ADCS can be increased. Furthermore, knowledge of the satellite magnetic field enables the PocketQube team to include magnetically sensitive payloads on future missions. These desires of the PocketQube team indicate that a magnetic measurement system is valuable.
Apart from the PocketQube team, a magnetic measurement system will likely also be valuable to other PocketQube designers who desire to implement a magnetically sensitive payload or who desire to optimize their ADCS.
Even though the current design of the measurement system focuses on measuring satellite and satellite subsystem magnetic field, this does not mean that it cannot be used for other DUTs. For many other electronic applications inherent electromagnetic interference (EMI) is a problem which needs to be tackled for the application to function as intended. To this end, quantification of the magnetic fields of components is essential. Given a few potential changes, the to be designed measurement system will also be able to conduct measurements regarding inherent EMI in products besides PocketQubes. The above reasons indicate that there will be a market for a working magnetic field measurement system.

An alternative to purchasing one's own magnetic field measurement system is to use an external facility for this purpose. The usage of such a facility brings along additional costs. Having an in house magnetic field measurement system voids the need for an external facility, and an own measurement system can be used repeatedly, without additional costs. Therefore it is expected that a commercial working magnetic field measurement system can be valued at several thousands of Euros.
It should be noted that before any commercial product will be produced, a proof of concept will first be developed. The budget for this proof of concept will be lower than the budget for a commercial product.
Based on the above arguments, and a discussion regarding the budget of the measurement system with Dr. Ir. J Bouwmeester, who has worked on the Delfi satellites extensively, the budget for the proof of concept has been defined. The target range for the cost of the proof of concept magnetic measurement system is 500 - 1500 Euros.

1.4 The target range for the cost of the magnetic field measurement system is 500 to 1500 Euros.

2.3. Supporting structure requirements

In this section the requirements related to the supporting structure of the measurement system are discussed.

2.3.1. System scalability

To keep the magnetometers in place on and/or around the DUT, a supporting structure is needed to which the magnetometers can be mounted. This supporting structure shall be designed in such a manner that the same measurement system can be used for different sizes of DUTs. The range of DUT size which shall be considered for this measurement system spans from a entire 3P PocketQube to an individual subsystem of a PocketQube. A 3P PocketQube, including sliding backplate and uncertainty margins, has dimensions of 192,1x51,7x50,1 mm (defined in [1]), this is also shown in Figure 2.1. The width and depth dimensions should all be increased by an additional 10 mm on each side to allow for any potential deployable components which might be present on the satellite surface (defined in [1]). The dimensions of different individual subsystems vary, but considering the fact that most subsystems are 'stacked' in the satellite, an approximate dimension of 50x50xh mm is expected, with h being the height of the subsystem. To cover this range of dimensions the measurement system will need to be scalable. For the supporting structure this means that it has to be able to hold both an entire 3P PocketQube, as well as one individual subsystem, in place. Also, the positions of interest for magnetic measurements will change depending on the (size of the) DUT. Thus the supporting structure has to allow for different magnetometer configurations, depending on the user's desired measurement positions. The moving range of the magnetometers shall at least be equal to the dimensions of the largest DUT, to allow the user to cover the whole of a 3P PocketQube. To allow for some room to safely put the DUT into its desired position, 10 mm is added to the moving range of the magnetometer on each side of the DUT. This brings the magnetometer moving range to atleast 212 mm regarding the height of the measurement system, and 91.6 mm for the width and depth of the measurement system. It should be noted that not all magnetometers are required to have such a large moving range. A magnetometer at the bottom of

the measurement system will hardly have to move when the DUT changes from a 3P PocketQube to a small subsystem (assuming both DUTs will be placed at the bottom of the measurement system).

2.1 The supporting structure shall be able to hold DUTs ranging from a 3P PocketQube (192x71,6x70 mm (uncertainty ± 0,1 mm)), to an individual subsystem (50x50xH mm), in place.

2.2 The measurement system shall have movable (by the user) magnetometers.

2.2.1 The moving range of the movable magnetometers shall be 212 mm regarding the height, and 91.6 mm regarding the width and depth of the measurement system.

2.3 The supporting structure shall keep magnetometers in place at different positions.

2.3.1 The measurement system shall provide information regarding the positions of the magnetometers which can directly be entered into data analysis software.

2.4 The system shall be usable without having to risk damaging the DUT.

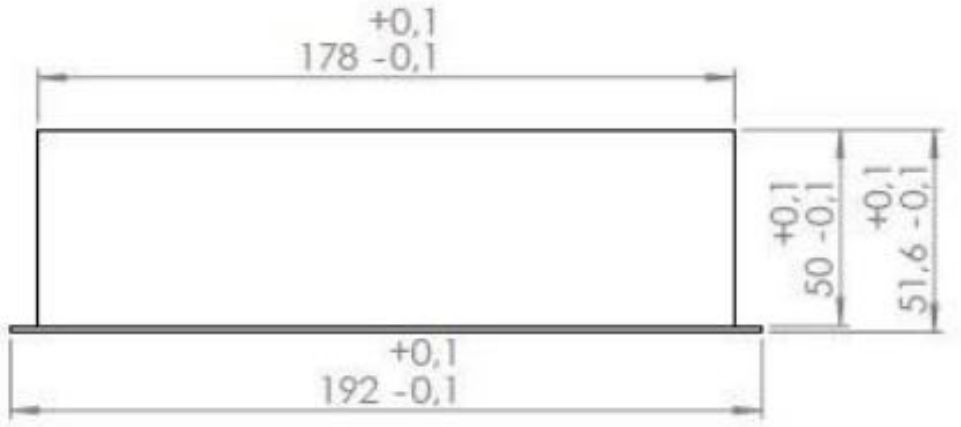

Figure 2.1: The PocketQube standard dimensions for a 3P PocketQube, excluding the 10 mm margins [1].

2.3.2. Magnetometer placement (perpendicular to DUT)

[Deleted]

2.3.3. Magnetometer placement (parallel to DUT surface)

When a magnetic field measurement is conducted, it is necessary to know to which positions w.r.t. the DUT the measured values correspond. Thus, it is important to be able to determine the position of the magnetometers w.r.t. the DUT with a certain accuracy. The desired spatial accuracy of the magnetometers will depend on the spatial variation of the DUT magnetic field, the smaller this spatial variation is, the better the spatial accuracy of the magnetometers needs to be. At the moment, not much is known regarding the spatial variation of DUT magnetic fields. So, a magnetometer spatial accuracy of 2 mm w.r.t. the DUT is chosen. This will be divided evenly over the placement of the DUT and the magnetometers.

2.6 The supporting structure shall facilitate magnetometer placement w.r.t. the DUT with an accuracy of 2 millimeter.

2.6.1 The supporting structure shall facilitate placement of the DUT at the desired location w.r.t the supporting structure with an accuracy of 1 mm.

2.6.2 The supporting structure shall facilitate magnetometer placement on the supporting structure itself with an accuracy of 1 mm.

The supporting structure is manufactured using a 3D printer. Requirement 2.6 will be verified by comparing the worst case 3D printer tolerances to the required accuracy. If the worst case 3D printing inaccuracies add up to a value lower than the required accuracy, requirement 2.6 is met.

2.3.4. Magnetometer measurement locations

For certain DUTs it is desirable to measure the magnetic field on all sides of the DUT. Taking an individual subsystem as an example, one might want to know how its magnetic field affects both the subsystem above and below it, as well as the solar panels surrounding it on the outside of the satellite. Thus, the supporting structure should facilitate measurements on all sides of the DUT.

2.7 The supporting structure shall facilitate measurements on all sides of the DUT.

2.4. Magnetometer requirements

In this section the requirements related to the magnetometers used in the measurement system are discussed

2.4.1. Magnetometer type

It is desired to measure the magnitude and direction of DUT magnetic fields, so the magnetometers selected for the measurement system should be vector magnetometers.

3.1 The magnetometers shall be able to measure the magnitude and direction of the magnetic field.

2.4.2. Magnetometer error

The next magnetometer requirement will be regarding the maximum allowed error for the magnetometer measurement result. The measurement error will consist of multiple different components, which will all be adressed separately in the list below.

- The target parameter of the measurement system is the DUT magnetic field. This is obtained by subtracting a background measurement from a measurement with the DUT. In essence, the system is thus measuring a step increase (or decrease), and the linearity (sensitivity of the magnetometers w.r.t. a field change) error will affect the measurements. The linearity error can be corrected for by calibration, but a residual linearity error will remain.
- For some magnetometers a temperature drift is known to influence their measurement results. This error can be several factors larger than the measured signal. This error therefore needs to be corrected for as much as possible, but an artifact is likely to remain.
- When the magnetometers are placed too close together, they can interfere with one another. This interference gives rise to an error in the measured signal. By placing the magnetometers further apart, this error can be reduced, but the spatial resolution of the measurement system as a whole suffers from this.
- Magnetometer precision refers to the spread in measured values of the same magnetic field. If the spread in measured values from the magnetometer is too large, it will not be possible to distinguish the measured magnetic field from the natural spread of the magnetometer results. To reduce the uncertainty, multiple measurements will be conducted, the average of which will be the measurement result. The error due to magnetometer precision will be quantified as the standard deviation of the mean, which is calculated using

$$\sigma_m = \frac{\sigma}{\sqrt{N}}, \tag{2.1}$$

  where N is the number of measurements and σ is the standard deviation of the N measurements in the same unit as σ_m, being nT. It should be noted that this error is also affected by (internal) noise.

To formulate a requirement for the maximum allowed error for the measurement system, the usage of *on board* magnetometers for ADC purposes is used. In Section 2.1 it has been determined that the maximum allowed error for onboard measurements (for the purpose of ADC) is 68 nT. To achieve this, the satellite magnetic field needs to be determined beforehand with an accuracy below 68 nT. As there will also be uncertainties present in the on-board magnetometer (e.g. its resolution), this number will be reduced by half, to allow for uncertainties during the on-board measurements. Thus, when taking ADC as defined in Section 2.1 as the purpose for doing measurements on a DUT, the cumulative error of the listed uncertainty inducing factors can be no larger than 34 nT. As the cumulative error of the items listed above is of interest, no individual error budget is assigned to each individual uncertainty from the list.

3.2 The cumulative error in magnetometer measurements shall be below 34 nT for each axis. The cumulative error is introduced by; the magnetometer residual linearity error, temperature drifts, magnetometer interference and magnetometer precision.

To verify requirement 3.2, different measurements will be conducted. The linearity error is corrected using a correction factor. This factor is found by exposing the magnetometers to a stepwise magnetic field increase over the magnitude of the maximal rated magnetic field (requirement 3.4). The difference in the measured step increase and actual step increase of the magnetic field will yield a correction factor for the linearity error. The residual linearity error is quantified by the standard deviation in the different linearity error correction factors found over multiple calibrations.
The error due to temperature drift will be tested by exposing the magnetometers to a constant magnetic field, whilst increasing their temperature. The drift of the measured magnetic field will yield the error due to temperature drift. For both the residual linearity and temperature drift test, errors due to (internal) noise and magnetometer resolution will also be accounted for.
To measure the error due to magnetometer interference, two measurements on a similar DUT are conducted. One with all magnetometers present, and one with a single magnetometer, the influence of magnetometer interference can be quantified by taking the difference between these measurements.
The magnetometer precision will be measured using a known constant magnetic field source, and conducting repeated measurements. The spread in these measurements quantifies the precision of the magnetometer. Also this test will be affected by (internal) noise.
Summing the above measured errors in the final measurement system yields the cumulative error, which can be compared to the required value.

2.4.3. Magnetometer spatial resolution

The placement of the magnetometers on the supporting structure will largely determine the spatial resolution of the measurement system. Placing the magnetometers close together yields a high spatial resolution, but placing them too close together might cause the magnetometers to interfere with one another, as they contain magnetic materials and a current runs through them. The above requirement encompasses the minimal distance between two magnetometers, as it depends on the other error inducing effects. The maximal distance between two magnetometers follows from the fact that it is desired to measure (potential) differences in the magnetic field at different locations on the DUT. To do this, atleast two magnetometers will be needed on one side of the DUT. Using the DUT sizes defined in Section 2.3, it is immediately noted that the smallest DUT size is unknown, as each individual subsystem can have a different height. Therefore the second smallest expected DUT size, being the horizontal dimension of a 1P PocketQube (i.e. one block of Delfi-PQ) will be used as the maximum allowed distance between two magnetometers. This distance shall thus at most be 50 mm.

3.3 Magnetometers can be placed within 50 mm from one another.

2.4.4. Magnetometer saturation

As the measurement system shall be suitable to measure the magnetic field of different DUTs, the magnetometers used in the measurement system should also be operational (and not saturate) in the magnetic field range of different DUTs. It is expected that the largest DUTs, 3P PocketQubes, will produce the largest magnetic fields. Therefore the required operational range will be based on the largest measured DUT field during the preliminary measurements. This was a measurement close to the battery pack of the Delfi-PQ 3P PocketQube, the measured field has a magnitude of approximately 5 µT. To account for different DUTs in the future, a margin is included to extend the required range of the magnetometers to [-10, 10] µT.
It is important to note that for unshielded measurements, the EMF will be present and dominating over any DUT field in this range. Therefore the operational range of the magnetometers in an unshielded scenario will depend largely on the magnitude of the EMF (~45 µT). In the worst case, where the EMF and DUT field align, this will result in a magnetic field of ~55 µT which needs to be measured. For unshielded measurements the operational range of the magnetometers thus needs to be 0-55 µT.

3.4 The magnetometers shall be operational in the magnetic field range of [-10, 10] µT if the EMF is nulled, and in the magnetic field range of [-55, 55] µT if the EMF is present.

Requirement 3.4 will be verified by exposing the magnetometers to a known field source. By bringing the magnetometer closer to the source, the measured magnetic field will increase until the magnetometer reaches its

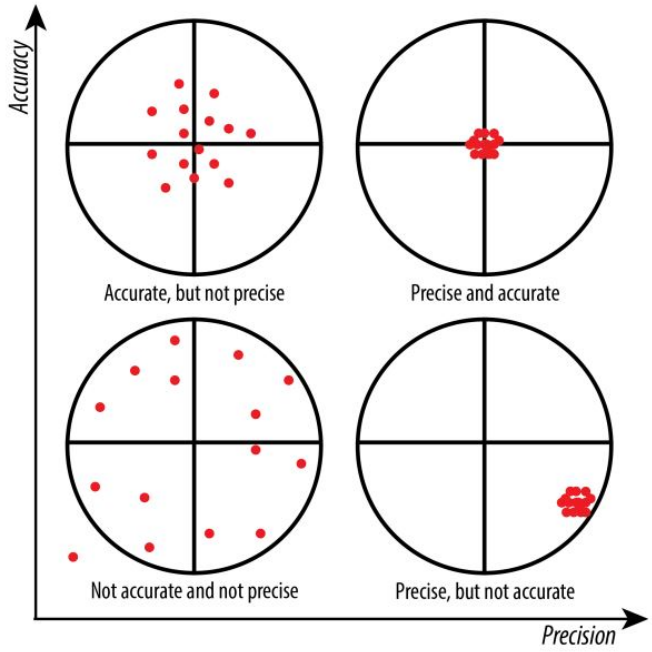

Figure 2.2: Comparison of the definition of precision and accuracy [2].

saturation point. Knowing the magnetometer saturation point enables one to verify that the magnetometer is operational in the range specified in requirement 3.4.

2.4.5. Magnetometer accuracy

The accuracy of a magnetometer refers to how close the magnetometer readings are to the actual magnetic field. In Figure 2.2 the difference between precision and accuracy is illustrated. To obtain a measurement result, a background measurement will be subtracted from the measurement with the DUT present. In this case, the accuracy of the magnetometers is of low priority, as a constant error will drop out in the subtraction (Note; a non-constant error falls in the precision category). For this reason no requirement will be placed on the accuracy of the magnetometers.

2.4.6. Magnetometer Frequency

One potential use of the measurement system is to investigate what part of the DUT magnetic field is static, and what part is dynamic. This information can be used to determine from what physical components the magnetic field contributions originate. To find the source of dynamic contributions to the magnetic field, a Fourier transform of the measurements can be made. Peaks in this transform correspond to a physical component which generates a magnetic field at a specific frequency. All contributions to the magnetic field which have a frequency below half the measurement frequency can be distinguished properly.
As it is currently unknown what frequencies can be expected, and as this can differ for each DUT, a magnetometer which can operate on multiple measurement frequencies is desirable. This enables the user to use the high frequency mode of the magnetometer for the purpose of finding which physical components contribute to the total field, and the lower frequency modes for improved resolution measurements.
Typical AC currents have a frequency of 60 Hz. According to the Nyquist criterion, a frequency in excess of 120 Hz is required to properly distinguish this peak in a Fourier transform. Including a small margin, the magnetometer should atleast be able to measure at a frequency of 150 Hz.

3.5 The magnetometer shall be able to measure with a measurement frequency of 150 Hz.

2.5. Data acquisition and processing

In this section the requirements related to the data acquisition and processing subsystem are discussed.

Data	Number of bits
Slave address, read bit, ACK	9
Start/Stop address	2
Data, ACK (8+1) x 3 x 3	81
Register pointer, Start/Stop (8+2)	10
Start/Stop data	2
Total	104

Table 2.2: The operations performed and bits needed in a read transaction.

2.5.1. Data acquisition

A microcontroller will be used to control the magnetometers. If one desires to adjust the magnetometer settings, a user interface is needed. For this purpose, a PC will be used on which the software programme used by the microcontroller can be altered, before uploading it to the microcontroller.
The output of the micro controller shall be data which is suitable for exportation to a different software, which is more suitable for data processing and analysis. Exporting the data live (as it is being measured) to a different software will also suffice. The software required to operate the magnetometers needs to be clear and well documented, such that an independent user can use it without additional help from the author.

4.1 An independent user needs to be able to operate the data acquisition software, without additional help from the author.

4.1.1 The software needed for data acquisition shall be commented in such a manner that the function of each line of code is transparent for an independent user.

4.1.2 In the software needed for data acquisition a clear distinction shall be present between what settings a user is supposed to change, depending on their preferences, and what settings are supposed to be left unchanged.

4.2 The output of the data acquisition software shall be a .csv or .dat file OR the data shall be exported live to a different software. One of these two methods will suffice.

It is important that the data acquisition method will not limit the magnetometer in its operation. This is important for both the sampling rate as well as for the resolution of the system.
For the resolution, the digital resolution of the system should be higher than the magnetometer resolution. This is required as a digital resolution which is *lower* than the magnetometer resolution would lower the effective resolution of the system. In requirement 3.2 the cumulative error is restricted to be below 34 nT, which includes the magnetometer resolution. Assuming the magnetometer resolution is responsible for half this cumulative error, the digital resolution of the data acquisition should be below 17 nT (i.e. 17 nT/LSB or 59 LSB/μT).
If the magnetometer sampling rate is too fast for either the microcontroller or the data acquisition software, the effective measurement frequency of the system will be lowered. To prevent this, the I2C baud rate and the time it takes the microcontroller to obtain a measurement need to be constrained. The required I2C baud rate can be estimated by using the I2C protocol described in the RM3100 datasheet [3]. The RM3100 is the magnetometer chosen in the magnetometer trade-off, described in Section 3.1. The I2C protocol describes the sequence needed to read data from the RM3100, and is shown in Figure 2.3. In Table 2.2 the operations and bits needed for one read transaction are listed. Note that one read transaction concerns the data from one magnetometer, for three axes. The data from one axis is stored in three separate sequential register addresses. The register address from which data is read is automatically incremented to n+1 by the RM3100 during the read transaction once the ACK from the microcontroller is received for register n. The result is that 104 bits are needed to read the data from one magnetometer. To read the data from four magnetometers with a frequency of 150 Hz a baud rate of 62.4 kHz is needed. This estimate does not account for clock stretching and pauses between transactions. The required baud rate should thus be well in excess of 62.4 kHz. The fast mode of the Raspberry Pi Pico, 400 kHz, is therefore selected as the required baud rate.
The data acquisition software will run in a loop to acquire the measurement data. If the time it takes to run this loop is longer than the inverse of the measurement frequency, the effective measurement frequency of the system will be brought down. In requirement 3.5 it is defined that the magnetometer needs to be able to

START	SLAVE ADDRESS							RW	ACK	DATA FROM REG. (N)							ACK	DATA FROM REG. (N+1)							NACK	STOP
S	A6	A5	A4	A3	A2	A1	A0	1	0	A7	A6	A5	A4	A3	A2	A1	A0	0	A7	A6	A5	A4	A3	A2	A1	A0	1	P

Figure 2.3: The I2C read protocol from the RM3100 manual [3].

operate at 150 Hz. So the loop in the data acquisition software which extracts the data from the magnetometer should last no longer than 6.6 ms.
To ensure that the data from each magnetometer will be read in the same order over each measurement, a data ready signal shall be used. This means that before reading a measurement, the data acquisition software will wait until all magnetometers give the ready signal. To ensure that no unnecessary time is lost in the data acquisition, the data ready signal pins will need to be checked with a frequency of atleast 1 MHz.
It is not required for the different magnetometers to be synchronized, as the data for each magnetometer is only relevant for the magnetometers own location.

4.3 The digital resolution of the data acquisition subsystem should be below 17 nT (i.e. 17 nT/LSB or 59 LSB/μT).

4.4 The baud rate of the micro controller shall be 400 kHz.

4.5 The data acquisition software shall need no longer than 6.6 ms total to read one measurement from all magnetometers.

4.6 The magnetometer data will be read using a data ready signal.

4.6.1 The data ready pins shall be checked by the microcontroller with a frequency of atleast 1 MHz.

4.6.2 A positive data ready signal shall be read by the microcontroller for each magnetometer, before the data of all magnetometers is read.

4.6.3 Each magnetometer shall give a data ready signal on a designated data ready pin when a measurement is conducted, which can be read by the microcontroller.

2.5.2. Data processing software

Data processing concerns translating the raw data into useful information. As different information might be useful for different users, the user needs to be able to change the output of the data processing software. For this reason, the software needs to be well documented, just like the data acquisition software.

4.7 An independent user needs to be able to operate the data processing software, without additional help from the author.

For each measurement, the user shall be able to define the desired measurement duration in the software. A data set for one measurement will include measurement data for the entire measurement duration, in 3 directions, for all magnetometers. As the magnetometers have different locations, the data for each magnetometer will be used separately in data processing. Thus, any output from the data processing is always linked to a certain magnetometer, and to a certain location.
The main purpose of the measurement system is to measure the magnetic field produced by the DUT at different positions (the positions of the magnetometers). Therefore the raw data, as well as the average measured magnetic field over the measurement duration will be part of the output (separately for each magnetometer). The average measured magnetic field will be calculated by taking the difference between the average measured magnetic field from a measurement with, and one without, the DUT present.
To obtain the uncertainty in the average measured magnetic field, the standard deviation of the mean will be used. The standard deviation of the mean will be calculated over the entire duration of the measurement, which can be chosen by the user. To quantify the influence of extreme values in the measurements, the kurtosis will be used. A positive kurtosis indicating a low influence of extreme outliers.
To give the user information of the range of magnetic field values which can be expected, two different ranges will be amongst the output. The maximum and minimum will be used to show the full range of measured

magnetic field values, but these can be influenced by heavy outliers in the data. Therefore the range of measured magnetic field values which fall within a 99.7% confidence interval will also be used. Both these values are corrected using the average background magnetic field.
For the standard deviation of the mean, kurtosis and field ranges each, a separate value will be calculated for the x-, y- and z-direction, as well as the total magnetic field. An example of the produced output in data processing is given in Table 2.3.
To give the user information about whether the DUT magnetic field is static or dynamic, a Fourier transform of the measurement data will be amongst the output. The peaks in the Fourier transform correspond to the frequencies which have the strongest contribution to the total magnetic field. Knowing these frequencies might allow the user to identify the origin of certain magnetic field contributions. The Fourier transform will be displayed graphically. The range of the Fourier transform will be half of the measurement frequency, due to the Nyquist criterion. For the frequency specified in Requirement 3.5 this means a Fourier spectrum ranging from 0 Hz to 75 Hz.
As in any measurement, there will be noise present in the measured data. To check whether this noise is white Gaussian noise the power spectral density of the measurement data will be used. If the PSD of the noise meets to following three criteria, the noise can be called white Gaussian;

1. the PSD is constant.
2. the PSD has a non zero variance.
3. the PSD has an auto correlation function which is nonzero only for n=0 (here n refers to the time difference between any two points in the PSD).

Criterion three is almost never met exactly, rather, the autocorrelation is very small for values of $n \neq 0$. Therefore the user will be provided with the necessary information to determine whether the three criteria for white Gaussian noise are met, so that one can determine this for oneself. This is done as for different purposes, the strictness on criterion 3 might vary. The following information will be amongst the output data for this purpose; the PSD of the measured noise (graphically), the variance of this PSD (graphically), the autocorrelation of the measured noise (graphically) and the lag value for which the autocorrelation drops below 0.1. This information will allow the user to determine whether the noise can be called white Gaussian noise.

4.8 The measurement duration shall be changeable by the user.

4.9 The output of data processing will contain the following elements:

- The raw and calibrated measurement data in each direction.
- Average measured magnetic field of the DUT in each direction.
- Standard deviation of the average measured magnetic field.
- Kurtosis of the average measured magnetic field.
- Maximum and minimum values of the measured magnetic field.
- Maximum and minimum values of the measured magnetic field corresponding to a 99.7% confidence interval.
- Fourier transform of the measured data ranging from 0 Hz to 75 Hz.
- The PSD and autocorrelation of the measured noise, both graphically displayed.
- The lag value for which the autocorrelation of the measured noise drops below 0.1.

4.10 Output will be separated by magnetometer locations.

4.11 Output will be separated in the x-, y- and z-direction, as well as a total value.

This concludes the defining of the system requirements. Research question 1, which reads, "What applications will a measurement system for small satellites have and what capabilities should such a measurement system have?", has been answered. The applications of the measurement system include the calibration of on board ADCS magnetometers and finding the locations of magnetic field sources in a small satellite. The capabilities the measurement system should have are in the requirements. The most important capabilities of the measurement system are to be able to measure with an uncertainty of 34 nT or less, and to be able to move magnetometers quickly and precisely.
The above requirements will be used in the design of the measurement system, and in the verification of said measurement system.

Direction	**X**	**Y**	**Z**	**Total**
Average measured magnetic field				
Standard deviation				
Kurtosis				
Full range				
99.7% confidence interval				
Lag value for 0.1 autocorrelation				

Table 2.3: An example of the data output produced in data processing. This output is given for each magnetometer.

3

Subsystem design

This chapter discusses the design of the three subsystems of the measurement system, being the magnetometers, the supporting structure and the data acquisition and processing software. For the magnetometers, a selection procedure is conducted to come to the best magnetometer choice. This is discussed in Section 3.1. The design of the supporting structure is discussed in Section 3.2. The working of the data acquisition and processing software is discussed in Section 3.3.

3.1. Magnetometer selection

In this section the magnetometers which will be used in the measurement system will be selected, this is done in three steps. Firstly, the selection criteria for the magnetometer are formulated, which is done in Subsection 3.1.1. Secondly, a list of possible magnetometers is established using the parametric search tools of five distributors. These magnetometers are then compared to the previously defined criteria in Subsection 3.1.2. Lastly Subsection 3.1.3 presents a more thorough analysis of the chosen magnetometer.

3.1.1. Magnetometer selection criteria

In this section the criteria for magnetometer selection will be formulated. These criteria have two functions. Firstly, they help in deciding which magnetometers of the initial list move on to the 'in depth' analysis. For this purpose the criteria can be seen as 'selection criteria'. If a magnetometer does not meet one of the criteria, it is immediately eliminated. Secondly, the criteria are the parameters on which the remaining magnetometers are scored in the trade off. The criteria will be based on the requirements defined in Chapter 2. If one of the criteria differs slightly from the requirements as listed in Chapter 2, a brief explanation will be given before the criterion is formulated. There are eight criteria in total, which will be addressed in the remainder of this section.

Criteria:

Requirement 3.1 states that "the magnetometers shall be able to measure the magnitude and direction of the magnetic field". The criterion related to this requirement is rather straightforward.

1 The magnetometer is a vector magnetometer.

Requirement 1.4 states that "the target range for the cost of the magnetic field measurement system is 500 to 1500 Euros". It is expected that the magnetometers will make up the largest chunk of the measurement system costs. It is not clear yet how many magnetometers will be needed for the measurement system, but it is expected that this number shall be somewhere in between 6 and 12. This number can depend on the cost and specification of the magnetometer. For example if a slightly more expensive magnetometer performs way better than a cheaper one, it is worth favouring quality of the magnetometer over quantity. Therefore magnetometers costing over 200 Euros will not be acceptable within the budget, and thus will not be investigated further.

2 The magnetometer costs 200 Euros or less.

Requirement 3.2 states that "the cumulative error in magnetometer measurements shall be below 34 nT". The cumulative error is introduced by; residual linearity error, magnetometer precision, temperature drifts, magnetometer interference and magnetometer precision". The error introduced by magnetometer interference depends on the placement of the magnetometers, and will thus not be included in the magnetometer criteria. For the magnetometer precision 34 nT will be the criterion, as a worse precision will inherently prevent requirement 3.2 from being fulfilled. In most datasheets for magnetometers precision itself is not mentioned. Instead, noise, noise density, noise floor or stability are often specified. These parameters all describe the fluctuation in different measurements of the same field, i.e. the precision. To be able to compare the different magnetometers to the precision criterion, the precision of a magnetometer will be expressed as the noise standard deviation (i.e. stability) of the magnetometer itself. For the magnetometer resolution the same criterion and similar reasoning as for the magnetometer precision applies. Establishing a magnetometer criterion regarding the temperature drift is a bit more cumbersome, as a temperature drift can be calibrated for. Therefore internal temperature compensation in the magnetometer will be seen as an advantage of the magnetometer, but its absence will not be a reason to discard a magnetometer immediately.

3 The magnetometer has a noise standard deviation of 34 nT or less.

4 The magnetometer has a resolution of 34 nT or better.

Requirement 3.3 states that "magnetometers can be placed within 50 mm from one another" (note that this regards the sensor in the magnetometer, not the edge of the IC-board). Next to this it is expected that approximately 1 cm is needed between the magnetometers to avoid interference. Therefore any magnetometer which has dimension which exceeds 40x40 mm shall not be investigated further. The height of the magnetometer is not restricted in the requirements, as long as the magnetic sensor is placed on top of the magnetometer (so it can be placed close to the DUT). But for the purpose of practicality any magnetometer with a height of more than 10 mm will be excluded from further investigation.

5 The magnetometer has dimensions of 40x40x10 mm or less.

Requirement 3.4 states that "the magnetometers shall be operational in the magnetic field range of [-10, 10] μT if the EMF is nulled, and in the magnetic field range of [-55, 55] μT if the EMF is present". At the moment it is not known whether the measurements will be conducted in the presence of the EMF or not. Therefore any magnetometer which has an operational range below [-10, 10] μT will be excluded from further investigation. Any magnetometer which has an operational range above [-10, 10] μT, but below [-55, 55] μT, will not be excluded from further investigation. But such magnetometers come with the limitation that they will only function when the EMF is nulled.

6 The magnetometer has an operational range of [-10, 10] μT or better.

It is desired that the magnetometer has been fully developed and is commercially available, as opposed to a magnetometer which is still in development.

7 The magnetometer is commercially available.

Lastly the interface of the magnetometer will be addressed. A digital magnetometer, which is already on a PCB, is preferred over an analog one. This voids the need of having to develop read-out electronics and a communication method for the magnetometer. Next to this, an I2C interface is preferred.

8 The magnetometer is a digital magnetometer with an I2C interface.

Requirement 3.5, regarding the magnetometer measurement frequency, is not used in the magnetometer selection criteria. The reason for this is that requirement 3.5 was only defined after the magnetometer selection was conducted. As the selected magnetometer features the option to select frequencies well in excess of 150 Hz, as defined in requirement 3.5, it is not expected that this requirement would have changed the outcome of the magnetometer selection.

3.1.2. Initial magnetometer selection

To come to a magnetometer which fulfills all eight criteria, the assortment of five different distributors has been looked into. The five distributors in questions are: Farnell, TTI, Digikey, Mouser and Amazon. As some of these distributors have an enormous assortment of magnetometers, the parametric search tool was used

to narrow down the list to magnetometers which were most likely to suit the purpose of this project. The parameters used for each distributor varied slightly, as not all distributors offer the same parameters within their search tool. The used parameters per distributor are as follows.

- **Digikey**:
  Category Linear, Compass. Interface (I2C AND/OR SPI), Axis (X,Y and Z) and Product status (Active).
  Category Magnetic field, Compass. Axis (X,Y and Z), Cost (<250 Euros) and Product status (Active).
- **Mouser**:
  Category Magnetic sensors. Type (3 Axis, AMR sensor, magnetometer).
- **Farnell**:
  Category IC Sensors, MEMS sensors. Availability (In stock) and Function (Tri-axis magnetometer).
  Category IC Sensors, MR Sensors. Availability (In stock).
- **TTI**
  Category Magnetic Sensors. Type (3 Axis, high sensitivity, Hall effect and magnetometer).
- **Amazon**:
  Category Sensors.

The magnetometers which came forward from the parametric searches are shown in Table 3.1. It should be noted that any magnetometer which shows up in the parametric search, but is not in stock, is not included in Table 3.1. Any magnetometer which showed up in the parametric searches of multiple distributors, has only been included once. The same goes for magnetometers which are similar, but are listed separately in the distributor's assortment due to packaging. All magnetometers shown in Table 3.1 have been compared to the criteria established in Section 3.1.1. Almost all magnetometers in Table 3.1 did not meet one or more of the eight criteria. The criterion which is failed is denoted in column three of Table 3.1, with only the last magnetometer, the RM3100, meeting all criteria.

3.1.3. RM3100 analysis

From the initial selection, only one magnetometer has come forward which meets all criteria. This is the RM3100, developed by PNI. In Table 3.2 the specifications of the RM3100 are denoted. These are the specifications as claimed by PNI in their RM3100 & RM2100 User Manual. These specifications are regarding the sensor including a breakout board. It should be noted that the given specifications are for a 200 cycle count, which limits the sampling frequency to 147 Hz.
Most of the specifications claimed by the manufacturer can be trusted beyond reasonable doubt, such as the dimensions and operational range. But it is desirable to check the performance of the magnetometer regarding the resolution and noise using additional sources.
Regoli et al. (2018) [3] have tested the RM3100 extensively to check its suitability for measuring low amplitude magnetic fields. Figure 3.1 shows the distribution of residual measurements over a 100 hour measurement series. It can be seen that the standard deviation of said measurements is 9 nT, which is in good correspondence with the noise (i.e. stability) claimed by the manufacturer. The resolution found by Regoli et al. (2018) [3] is 8.7 nT. This is above the digital resolution of the instrument, which is 3.3 nT. This difference is attributed to internal noise. Overall, Regoli et al (2018) [3] conclude that the performance of the RM3100 is excellent, and promising for the measurements of low amplitude magnetic fields.
The good correspondence between specifications claimed by the manufacturer and specifications found from tests gives no reason to doubt the claims made by PNI Sensor. As the RM3100 meets all criteria defines in Section 3.1.1, and is the only one that does so, it is the magnetometer of choice for the to be designed measurement system.

Magneto-inductive sensors

It should be noted that in this section, the magnetic flux intensity H is used, instead of the magnetic flux density B, which have units A/m and T respectively. This is done as the magnetic field in a material with magnetic properties is the subject of discussion in this section. The output of the RM3100 magnetometer is the regular magnetic flux density B that is used throughout the rest of this thesis.
The RM3100 magnetometer operates based on 3 individual magneto-inductive (MI) sensor elements, one

Distributor	Sensor model	Reason for exclusion
Farnell	SM353LT [27]	Not triaxial
	SM351LT [27]	Not triaxial
	SS552MT [28]	Not triaxial
	BM1422 [29]	RMS noise 116 nT, Resolution 42 nT
	MTI-1-0l-T [30]	RMS noise 50 nT
	MTI series (remainder)	>250 Euros
	ICM-20948 [31]	Resolution 150 nT
TTI	TCS40DLR/DPR [32]	Not triaxial
	HGDEPT021B [33]	No vector magnetometer
	LMPC0000	Too big (cylinder with height of 8 cm)
Digikey (Category: Linear, Compass)	MMC34160PJ [34]	150 nT RMS noise
	BMM150 [35]	Resolution ~300nT
	LIS2MDCTR [36]	Resolution 150 nT, RMS noise 300 nT
	AK09973D [37]	Resolution 1.1 µT
	LIS3MDLTR [36]	RMS noise 320 nT
	TLE493D-W2B6 [38]	Resolution 47.5 µT
	TLE493D-A2B6 [39]	Resolution 47.5 µT
	LIS2MDLTR [36]	RMS noise 300 nT
	MMC5633NJL [40]	200 nT RMS noise
	TLV493D-A2BW [41]	Resolution 32 µT
	MMC5603NJ [42]	RMS noise 200 nT
	ALS31313 [43]	Resolution 25 µT or worse
	AK09915 [44]	Resolution 150 nT
	AK09918 [45]	Resolution 150 nT
	MLX90392 [46]	Resolution 135 nT
	TLE493D-P2B6 [47]	Resolution 47.5 µT
	MMC3630KJ [48]	RMS noise 200 nT
	TMAG5273A2QDBVR [49]	Resolution 1.2 µT
	MLX90363 [50]	Resolution 4.9 µT
	TMAG5273A1QDBVR [51]	Resolution 1.2 µT
	MLX90395 [52]	Resolution 2.5 µT
Digikey (Category: Compass, Magnetic field)	HMC6343 [53]	Not in stock
	USB2xxxx	>270 Euros, probe over 20 cm
Mouser	MRMS205A-001 [54]	Not triaxial
	SM45xR [55]	Not triaxial
	MRSS29DR [56]	Not triaxial
	MLX90397 [57]	Resolution 750 nT
	MMC5893MA [58]	RMS noise 40 nT
Amazon	RM3100 [59]	Good

Table 3.1: The available magnetometers from five different distributors, in column three the criterion which is failed is mentioned.

Parameter	Specification (for 200 cycle counts)
Cost	24 Euros (directly from PNI)
Noise (Standard deviation)	15 nT
Resolution	13 nT
Dimensions	25.4 x 25.4 x 7.1 mm
Operational range	[-800 800] µT
Interface	I2C and SPI

Table 3.2: The specifications of the RM3100. All specifications are taken directly from PNI RM3100 User Manual and are regarding the sensor including the breakout board [3].

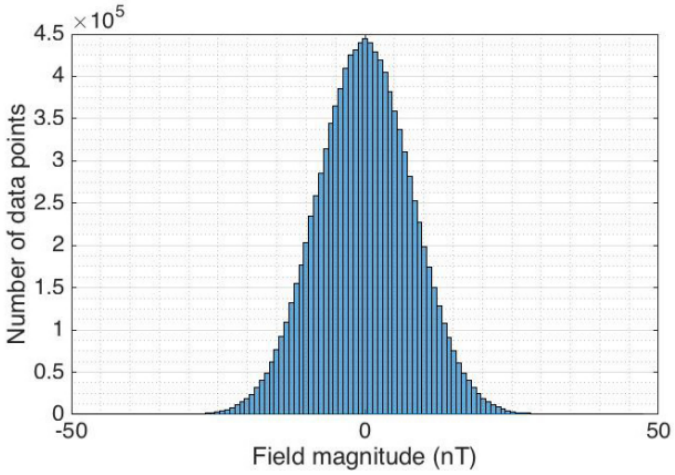

Figure 3.1: Distribution of stability measurements using the RM3100 [3].

for each spatial direction. Each MI sensor is part of an LR-oscillator circuit using a Schmitt trigger [60, 4, 3], as shown in Figure 3.2. The waveforms of said circuit are shown in Figure 3.3, the current I follows the same waveform as the voltage at location A, save for a constant scaling factor. The magnetic field H which is measured by the MI sensor is a combination of the ambient magnetic field, denoted as H_e, and the field generated by the current I, which is a constant times I

$$H = H_e + cI, \tag{3.1}$$

where H and H_e have the unit A/m and I has the unit A. The MI sensors consist of a solenoidal coil which is wrapped around a highly permeable material, the inductance of which varies depending on the applied magnetic field. This dependency is shown in Figure 3.4. As the current oscillates (following the lower waveform in Figure 3.3), the magnetic field felt by the MI sensor oscillates as well, according to the second term in Equation 3.1. The result of which is that the inductance of the highly permeable material inside the MI sensor will also oscillate between two points on the graph shown in Figure 3.4 (note, inductance is given by μ in this figure). Figure 3.4 shows said scenario for both a negative and positive voltage bias on the Schmitt trigger. It can be seen that the period of one oscillation (τ_p and τ_n) takes an equal amount of time for both the positive and negative bias.
Figure 3.5 shows what happens when an external magnetic field, H_e, is applied parallel to the MI sensor. The external field causes both the positive and negative regimes to shift to one side of the inductance graph. As an effect, τ_n becomes smaller than τ_p. The time it takes a set number of oscillations, this amount is called the cycle count, is measured for both the positive and negative bias, and subtracted from one another. From this difference the strength of the external magnetic field can be derived. The direction of the external field is found from whether τ_p or τ_n is larger [60, 3, 4].

This concludes the chapter on the magnetometer selection. Now that the RM3100 has been selected, it needs to be integrated with the supporting structure and data acquisition and processing subsystems. Calibration of the RM3100 is an essential part of the magnetometer subsystem, and will be discussed in Chapter 4.

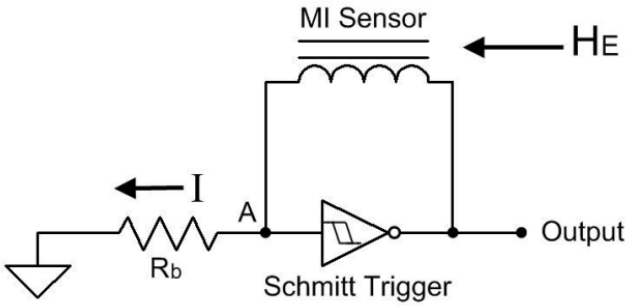

Figure 3.2: The L/R oscillation circuit and MI sensor used in the RM3100 magnetometer [4].

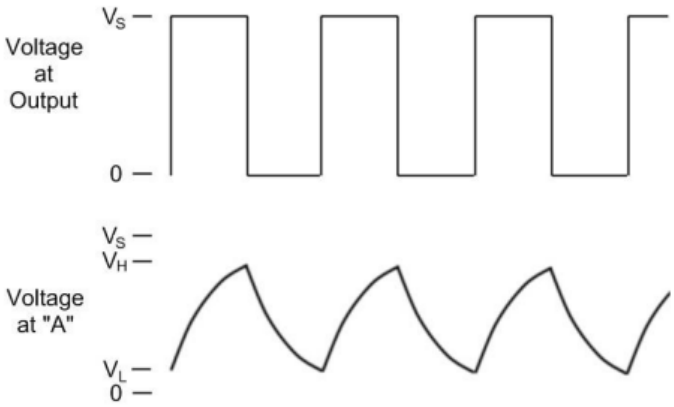

Figure 3.3: The waveforms of the L/R oscillation circuit shown in Figure 3.2 [4].

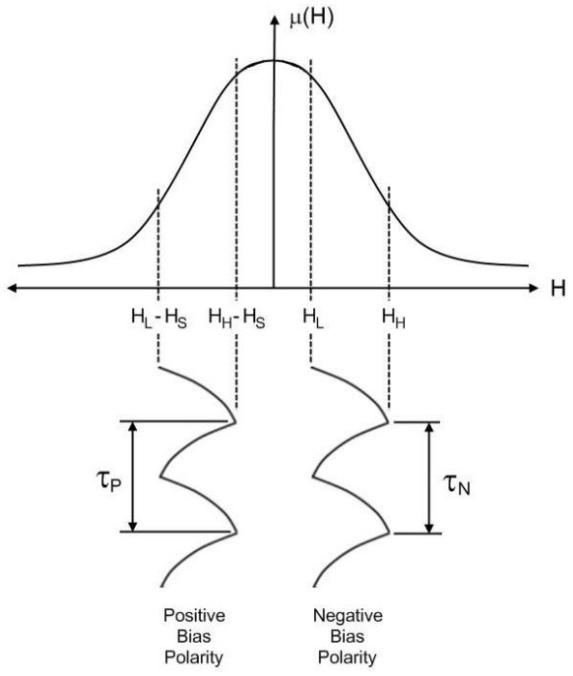

Figure 3.4: The sensor permeability as a function of the magnetic field and the circuit operation without an external magnetic field [4].

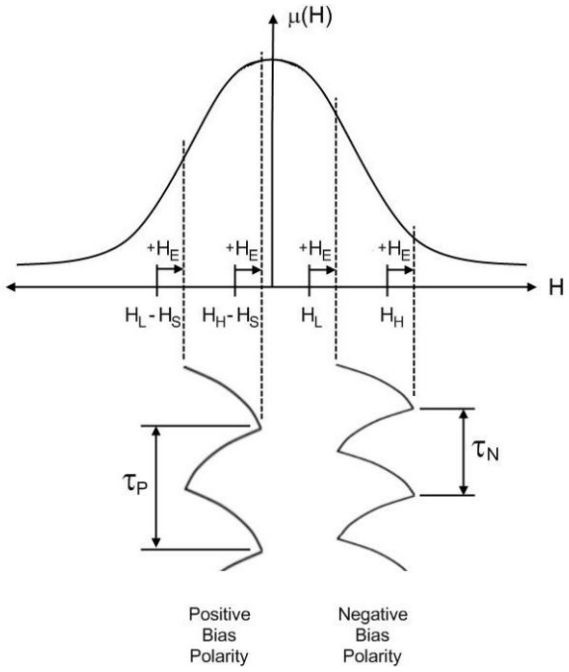

Figure 3.5: The sensor permeability as a function of the magnetic field and the circuit operation with an external magnetic field [4].

3.2. Supporting structure design

In this section the supporting structure design is discussed. The function of the supporting structure is to keep the magnetometers fixed in place at their desired location with respect to the DUT. Between measurements, the supporting structure should facilitate quick translation of the magnetometers, in all three spatial directions, as well as a convenient method of denoting the position of each magnetometer with respect to the DUT.
The supporting structure consists of 4 horizontal walls, a bottom and a top plate. Figure 3.7 shows the bottom plate, with two horizontal walls. The DUT is to be placed in the middle of the bottom plate, making it equidistant from each horizontal wall. To meet requirement 2.1, "The supporting structure shall be able to hold DUTs ranging from a 3P PocketQube (192x71,6x70 mm (uncertainty ± 0,1 mm)), to an individual subsystem (50x50xH mm), in place", the supporting structure is designed to be modular. The horizontal walls are split in two parts, such that the height of the supporting structure can be altered.
To meet requirement 2.2, "the measurement system shall have movable (by the user) magnetometers", the magnetometers are placed in magnetometer holders. The magnetometer holder, shown in Figures A.4 to A.7, consists of a main body and a side plate. Once the magnetometer is placed in the main body of the magnetometer holder, the main body and side plate can be slid into the rails segments on the horizontal walls, bottom and top plate. Additionally, the magnetometer holders ensure that the magnetometers can be positioned parallel to the wall segments despite the wires connected to the back of the RM3100, shown in Figure 3.6. Taking the magnetometer holder shown in Figure 3.7 as an example, it can be seen that the rails segment allows translation in the y-direction. Using the distance holders, shown in Figure A.11, the magnetometer holder is fixed in place. Translation in the x-direction is possible by using a magnetometer holder with a different thickness. In the z-direction, the magnetometers can be translated in increments of 38 mm by placing them in a different rails segment. Finer translation in the vertical direction is done by placing 1 mm thin plates below the DUT, to elevate the DUT w.r.t. the magnetometers.
The position of each magnetometer w.r.t. the DUT is thus fully determined by the magnetometer holder thickness, the distance holder used, the rails segment and the amount of thin plates used. These values are easily entered into the data analysis and processing software, to meet requirement 2.3.1, "the measurement system shall provide information regarding the positions of the magnetometers which can directly be entered into data analysis software".
The dimensions of the different components are shown in Appendix A. To ensure that requirement 2.4, "the system shall be usable without having to risk damaging the DUT", is met, a margin of 10 mm on top of the largest DUT size is included on each side.
To meet requirement 2.6, "the supporting structure shall facilitate magnetometer placement w.r.t. the DUT with an accuracy of 2 millimeter", a 3D-printer with tolerances of 0.2 mm is used. As the material used for 3D-printing is PLA, requirement 1.2, "no magnetic materials shall be used in the supporting structure of the measurement system", is also met.

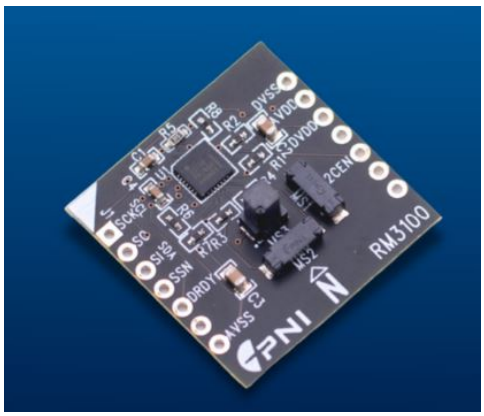

Figure 3.6: The RM3100 magnetometer.

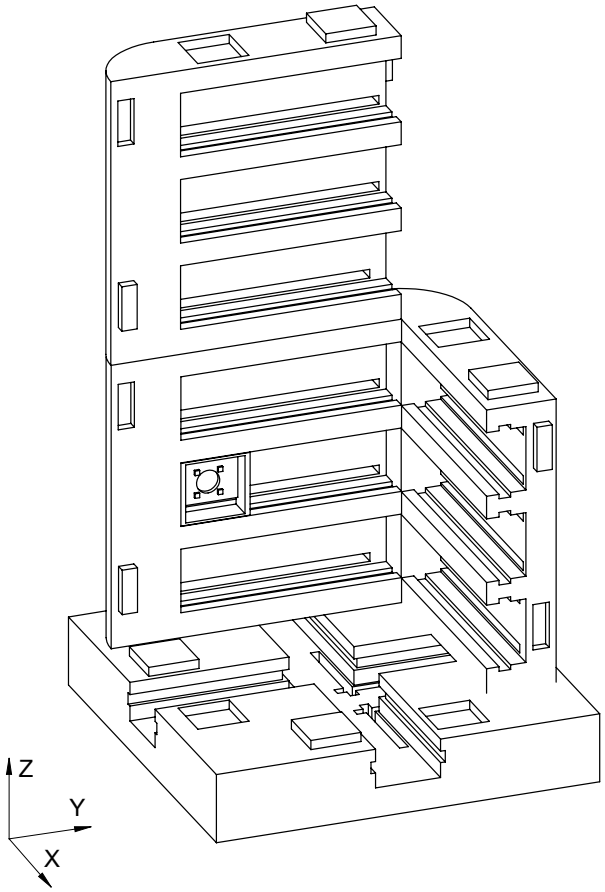

Figure 3.7: 3D drawing of the full measurement system, including three horizontal walls, the bottom plate and one magnetometer holder.

3.3. Data acquisition and processing

In this section the working of the data acquisition and processing software and hardware is discussed. The data acquisition software mainly acts as the interface between the user and the magnetometers. The user can start measurements and change magnetometer settings in the data acquisition software. The data processing software mainly functions to extract the raw measurement data from the magnetometers in the measurement system, and translate it into useful output. The data acquisition software and data processing software will be discussed separately in Subsections 3.3.1 and 3.3.2 respectively. In addition to discussing the data acquisition software, Subsection 3.3.1 will also discuss the hardware needed for data acquisition.

3.3.1. Data acquisition

For the data acquisition, a basic laptop is used. The laptop is connected to a microcontroller, in this case the Raspberry Pi Pico, as shown in Figure 3.8. The connection shown is repetitive for additional magnetometers, which are all linked to their own DRDY pin and to separate addressing pins (SA0 and SA1). The Raspberry Pi runs the data acquisition software, which is an Arduino IDE script based on an example by a Github user known as 'hnguy'[1]. Magnetometer settings are given as input by the user in the Arduino script, which is uploaded to the microcontroller before a measurement. During a measurement series, each magnetometer sets their own DRDY pin to high when a measurement is ready. Once all DRDY pins are high, the Raspberry Pi reads out all the data, converts it from bits to magnetic field values, and sends it to the laptop. The I2C baud rate is 400 kHz, corresponding to the fast mode of the Raspberry Pi Pico. Once the data is read from a magnetometer, its DRDY pin is automatically set to low, and the next measurement is conducted. Using Matlab, the data coming from the Raspberry Pi is stored in a .mat file on the laptop, so that it can be used in data processing after the measurement series. The measurement duration is specified in the Matlab script. Figure

[1] URL: https://github.com/hnguy169/RM3100-Arduino (Date of access 24-01-2023)

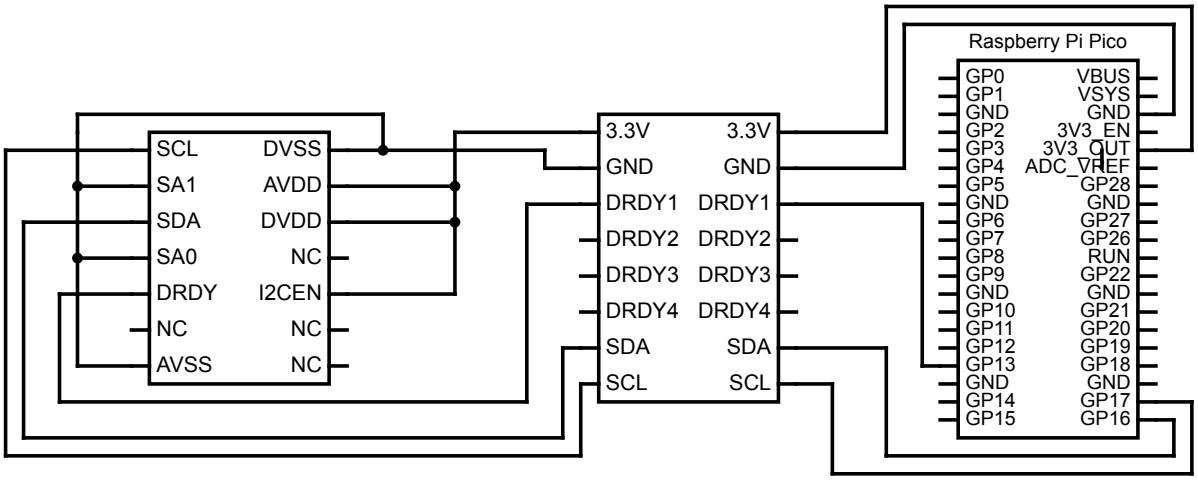

Figure 3.8: The circuit used for the data acquisition. The magnetometer, breadboard and Raspberry Pi Pico are shown from left to right.

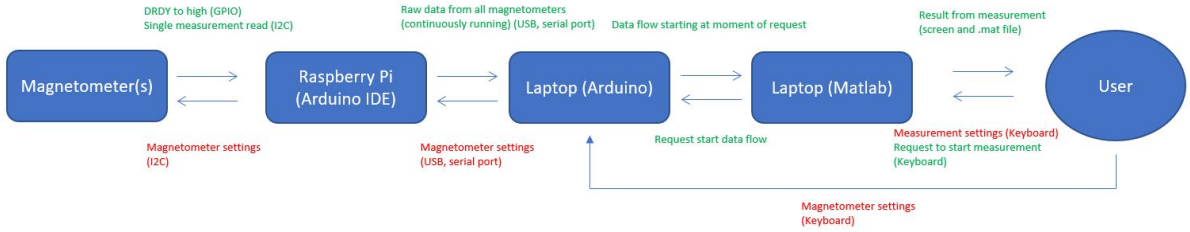

Figure 3.9: Data flow diagram showing the different components used in the system, and the flow of data between them.

3.9 shows the above described dataflow schematically. All communication before the start of a measurement is shown in red, communication during a measurement is shown in green.

3.3.2. Data processing

The purpose of data processing is to take the .mat file stored by the data acquisition software, and translate it into useful information for the user. Requirement 4.9 specifies what should be amongst the output of the data processing software.

The data processing software requires two input files from the user. One file with the measurement data, and one file with background measurement data. The user should also input the magnetometer positions, such that they can be graphically displayed by the data processing software. Lastly, the user has to provide the calibration factors for each axis of each magnetometer, found during the calibration procedure as described in Chapter 4.

Once the necessary input is provided, the data processing software shows the desired output as follows. The desired output which is in the form of a value is grouped per magnetometer in a table, as shown in Figure 3.10. The raw and calibrated measurement data is saved alongside the tabulated output, but is not displayed by default. The graphical outputs are displayed as well as saved. Figures 3.11 and 3.12 show the side and top view of the magnetometer positions w.r.t. the DUT during a sample measurement. Figure 3.13 shows the Fourier transform of the same sample measurement. The power spectral density and autocorrelation of the same sample measurement are shown in Figures 3.14 and 3.15.

The Fourier spectrum shown in Figure 3.13 is normalized w.r.t. the DC peak. It can be seen that between 1 Hz and 18 Hz the spectrum is below 0.1% of the DC peak value, meaning that no dynamics are observed in this measurement between 1 Hz and 18 Hz.

Using Figures 3.14 and 3.15 one can determine whether the noise present in the sample measurement is white Gaussian. For this, the three criteria mentioned in Subsection 2.5.2 need to be met.

1. The PSD is constant.

2. The PSD has a nonzero variance.

3. The PSD has an auto correlation function which is nonzero only for n=0 (here n refers to the time difference between any two points in the PSD).

From Figure 3.14 it can be seen that criteria 1 and 2 are met, as the PSD is approximately constant and has a nonzero variance. Criterion 3 can be determined graphically as well as using the lag value shown in Table 3.10. It is evident that the autocorrelation shown in Figure 3.15 is not nonzero for values of $n \neq 0$, which means that the noise is correlated in time. An explanation for this could be magnetic fluctuations due to environmental sources. As the autocorrelation peaks sharply at n = 0, the noise in this sample data can be approximated as white Gaussian.

	Average DUT field [μT]	Standard Deviation [μT]	Kurtosis	Full Range		99.7% CI		Lag Value
x-direction	-0.73045	0.0018607	4.9382	-1.3685	-0.32912	-1.287	-0.42083	-3636
y-direction	-1.1646	0.0014194	3.254	-1.5642	-0.69175	-1.4578	-0.81943	-116
z-direction	0.86183	0.0013967	3.4013	0.39013	1.2181	0.50541	1.1342	-3572
total	1.6225	0.0027254	2.9382	-1.5859	-0.71839	-1.4997	-0.85143	0

Figure 3.10: The output of the data processing software (for M1).

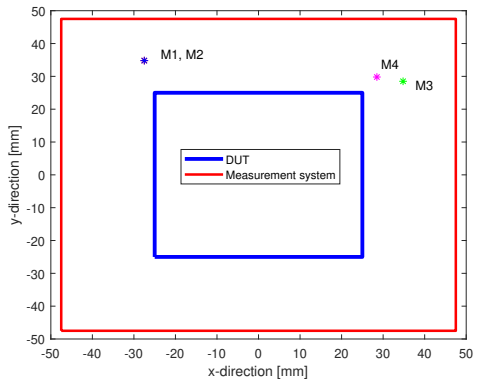

Figure 3.11: Topview of the magnetometer locations around the DUT for configuration 1.

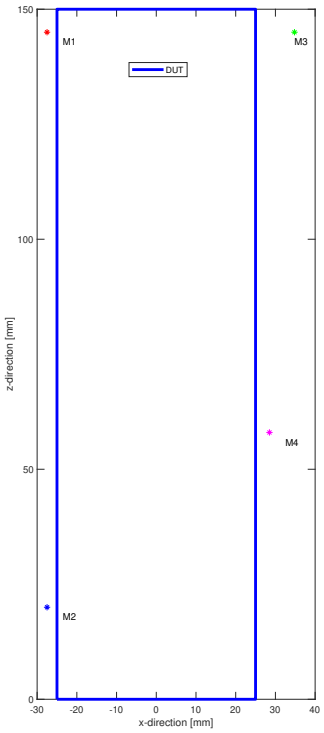

Figure 3.12: Sideview of the magnetometer locations around the DUT for configuration 1.

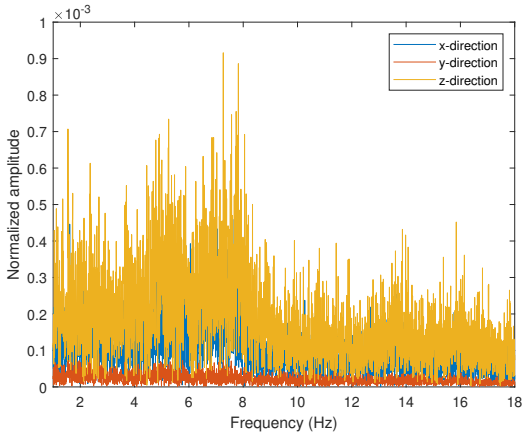

Figure 3.13: The Fourier transform of the sample measurement data, part of the data processing subsystem output.

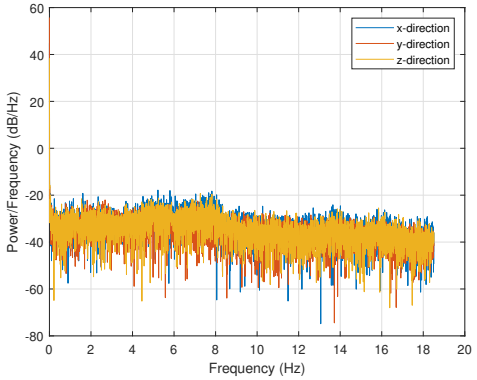

Figure 3.14: The power spectral density of the sample measurement data, part of the data processing subsystem output.

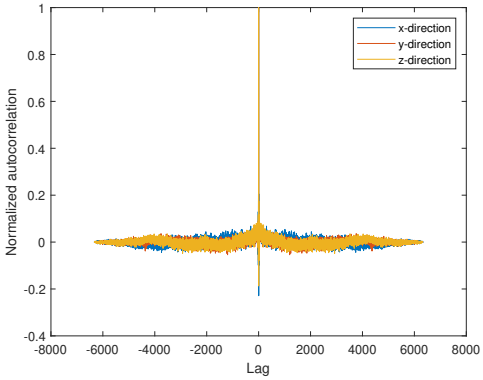

Figure 3.15: The autocorrelation of the sample measurement data, part of the data processing subsystem output.

4

Magnetometer calibration

In this chapter the calibration of the RM3100 magnetometers is discussed. In the final system, the magnetometers will be used to measure the difference in magnetic field with and without a DUT present. Therefore it is important that the magnetometer linearity is properly calibrated, whereas a potential constant offset is not relevant. To calibrate the linearity of the magnetometer, a Helmholtz coil (HC) system is used. Section 4.1 will discuss the Helmholtz coil system. Section 4.2 will explain the calibration method used, and Section 4.3 will discuss the results of the calibration.

4.1. Helmholtz coil system

A Helmholtz coil (HC) system, as illustrated in Figure 4.1, is used to calibrate the RM3100 magnetometers. The purpose of a HC system is to create a uniform magnetic field at the location marked z = 0 in Figure 4.1 by running the same current I through two similar coils of N turns each. The coils are separated by a distance d, which corresponds to twice the coil radius R. By increasing the current through the coils step by step, the magnetic field at the center of the HC system can be increased step by step as well. The magnetic field at the center of the HC system is described by [5]

$$B = \frac{8\mu_0 IN}{5\sqrt{5}R}, \tag{4.1}$$

where μ_0 is the vacuum permeability of $1.256\,\mu\text{NA}^{-2}$, R the coil radius in m, N the number of turns per coil and I the current in A. The magnetic field created by the coils at the center of the HC system only has a component in the z-direction.

To calibrate the magnetometer linearity the current through the coils is gradually increased, and the change in magnetic field is measured using the magnetometer. This measured change is compared to the expected change, which is calculated using Equation 4.1. This method works well if the HC system used for the calibration is 'perfect'. The HC system used for this calibration is not perfect, as the lower coil has one winding more than the upper coil. Besides this, the sensor is not placed in the exact middle point of the coils. These two effects ensure that the real field produced by the HC system is not exactly similar to the field described by Equation 4.1.

To test the performance of the Helmholtz coil, a different magnetometer is used. This is a magnetoresistive milligauss meter by AlphaLab, which is placed in the middle of the HC system. The magnetic field is then increased stepwise. Figure 4.2 shows the measured magnetic field change for different currents as blue circles, with the expected magnetic field for a 'perfect' HC system from Equation 4.1 in orange. It can be seen that the measurement points follow the expected trend well. The ratio between the gradient of the measured data and the expected data is 1.042, meaning that the real HC system depends slightly stronger on the current than a perfect HC system would. As the remainder of the calibration will be carried out using an imperfect HC system, the expected magnetic field for the RM3100 calibration will be based on the measured magnetic field dependency of the HC system. I.e., the expected magnetic field of the HC system will be as described in Equation 4.1, multiplied by the correction factor 1.042, yielding

$$B = 1.042\frac{8\mu_0 IN}{5\sqrt{5}R}. \tag{4.2}$$

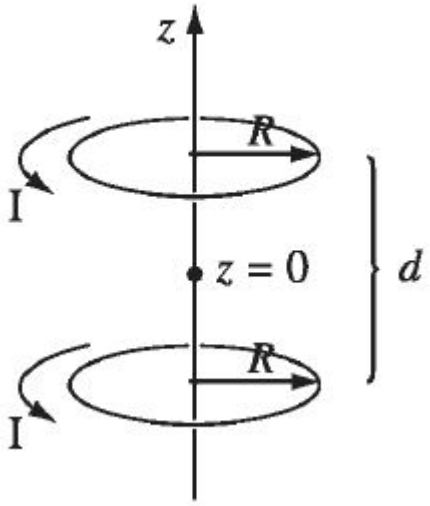

Figure 4.1: Helmholtz coil design, adapted from [5].

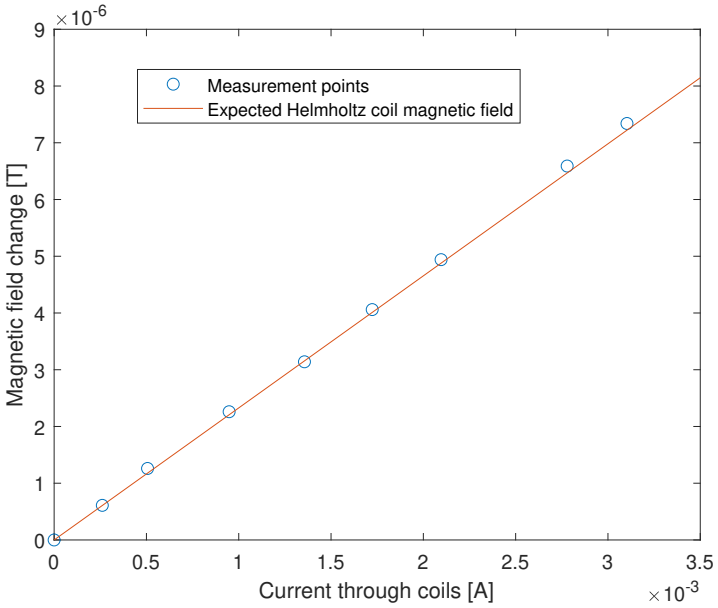

Figure 4.2: The expected and measured magnetic field change in the HC system for different coil currents.

4.2. Calibration method

To calibrate the magnetometers, they are placed in the center of the HC system, and the current through the coils is increased stepwise. For different current values, a measurement is made, which can in turn be compared to the expected magnetic field, which is calculated from Equation 4.2. Each measurement will consist of 363 individual measurements, made with a frequency of 37 Hz, over which is averaged. The uncertainty will be the standard deviation of the mean, as defined in Equation 2.1. Only the magnetic field in the z-direction, as shown in Figure 4.1, is used, meaning that calibration has to be done separately for each axis. Figure 4.3 shows the results of this measurement, with once again the measured points in blue and the expected HC field (with correction factor) in orange. It should be noted that error bars in Figure 4.3, which are defined as

the standard deviation of the mean, are in the order of 8 nT and thus invisible in Figure 4.3. From Figure 4.3 it can be seen that the RM3100 magnetometer used for this measurement is not sensitive enough, and thus needs correcting. The ratio of the gradient of the measurement points and the gradient of the real HC field is 1.014, which is thus the correction factor for this specific magnetometer's x-axis, as this magnetometer axis is aligned with the z-axis of the HC system. Note that this is a different correction factor than the one mentioned previously, which corrected for the HC system imperfections.
Ideally, this calibration procedure is conducted multiple times for each magnetometer axis, resulting in a series of normally distributed correction factors. The average of these correction factors is used to correct for the linearity error, and the standard deviation of these correction factors is the residual linearity error. In this calibration procedure, the measurements were only conducted in duplo. Table 4.1 shows the linearity errors of both measurements in columns 2 and 3 respectively, with the average correction factor in column 4. The residual linearity error is shown in column 5, all values have been separated per magnetometer axis.
The correction factor is to be applied as follows. One first conducts a measurement in an empty environment, to quantify the background field. Following this, the measurements on the DUT are conducted, from which the background magnetic field is subtracted. The resulting numbers are multiplied using the correction factors given in Table 4.1. This yields the calibrated measured magnetic field values. The uncertainty due to residual linearity error is found by multiplying the DUT magnetic by the residual linearity error percentage as given in Table 4.1.

4.3. Calibration results

The result of the calibration procedure is that the average linearity error for each axis is corrected for. Figure 4.4 shows the raw and calibrated data of one measurement series, along with the expected magnetic field. It can be seen that the calibrated data lies much closer to the expected magnetic field than the raw data, but an average (over all magnetometer axes) residual linearity error of 0.8% remains. Thus a DUT magnetic field of 10 µT will be measured with a standard deviation of 80 nT as an effect of residual linearity error. To reduce this residual linearity error, three suggestions are made to improve the calibration procedure.

- Figure 4.5 shows the raw data points for measurement series 1 and 2 for one of the magnetometer axes. The measurements were conducted under similar circumstances, yet the gradient differs by 4.7%. It is suspected that this is an artifact of the Helmholtz coils heating up over the course of the calibration procedure. Due to the coils being surrounded with isolating material, their temperature cannot be checked.
  To correct for this, the time between measurements has been increased. The effect of this is that the gradient difference between two similar measurement series decreased, which reduced the residual linearity error to an average of 0.8%. Reducing the time between measurement even more increases the likelihood of environmental magnetic field drifts interfering with the measurements.
  To reduce the residual linearity error even further, a more advanced HC system is recommended. Said HC system should remain at a constant temperature.
  Another potential explanation for the observed gradient difference is environmental magnetic field drift. This has been tested by conducting a measurement of longer duration without the HC system being operational. Over a time period of 135 s a drift of 5 nT has been observed. This is small enough to conclude that environmental magnetic field drift is not responsible for the difference in gradient shown in Figure 4.5.

- Figure 4.6 shows the Fourier spectrum of one of the calibration measurements. A clear peak is visible in the spectrum at a frequency of 11.5 Hz. This peak indicates a dynamic magnetic field source being present, either in the environment or in the HC system. As the same peak is visible in the longer measurement of 135 s, mentioned previously, it can be concluded that the 11.5 Hz source is part of the environment.
  It is expected that this peak influences the calibration, as the change in magnetic field is no longer purely due to the changing current in the HC system. This issue can be resolved by carrying out the calibration in a different environment, where this or other noise sources are not present.
  It should be noted that prior to the calibration procedure test measurements were carried out, and the 11.5 Hz peak was not observed at the time. It is assumed that the source producing this peak was switched on during the calibration procedure.

- The current calibration procedure features only two measurement series per magnetometer axis. This

is not a robust data set and is not enough to call the distribution of correction factors normal. More measurement series per magnetometer axis will yield a more robust normal distribution of correction factors (assuming the above two recommendations have been taken into account). Therefore, the standard deviation of this dataset *will* change as the number of measurements increases, whereas for a normal distribution, it should remain constant.

The above three recommendations can be used to decrease the remaining 0.8% in the residual linearity error. As this has not been done in this project, the residual linearity error remains at 0.8%.

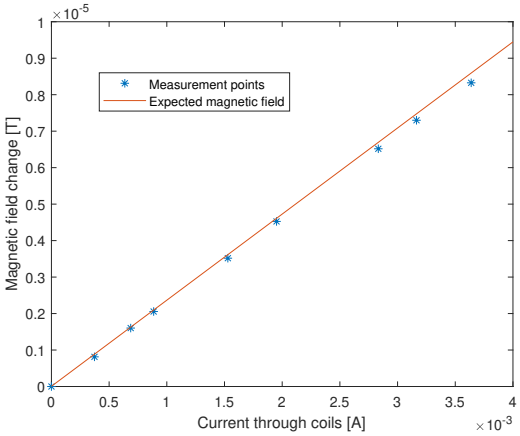

Figure 4.3: The expected and measured magnetic field change in the HC system for different coil currents using the RM3100 magnetometer.

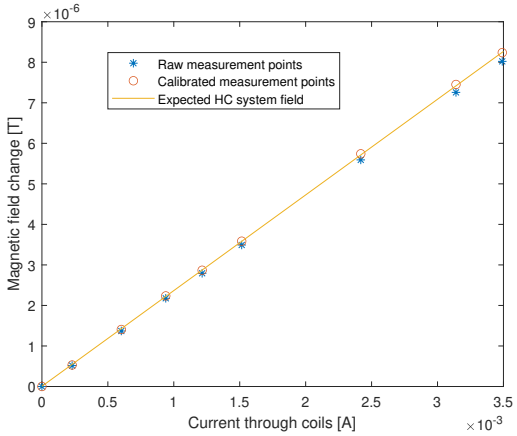

Figure 4.4: The orange line shows the expected HC system magnetic field for different currents. The blue and orange points show the raw and calibrated measurements.

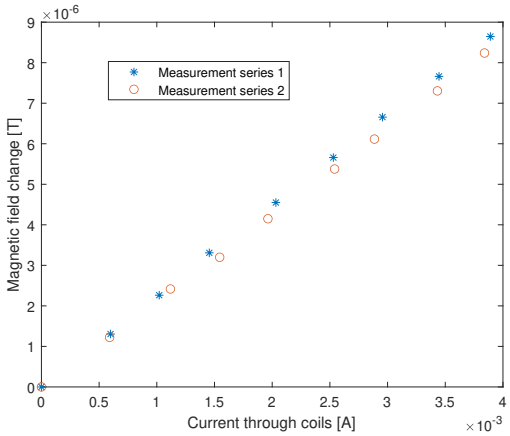

Figure 4.5: Measurement series 1 and 2, which were obtained under similar circumstances yet have a different gradient.

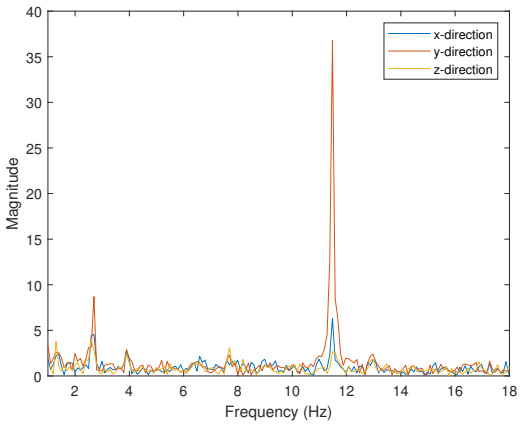

Figure 4.6: The Fourier spectrum of one of the measurements performed during the calibration.

Magnetometer (axis)	Linearity error meas 1 [%]	Linearity error meas 2 [%]	Correction factor	Residual linearity error [%]
M1 (x)	1.4	2.4	1.9	0.7
M1 (y)	6.7	6.1	6.4	0.4
M1 (z)	5.8	3.9	4.8	1.3
M2(x)	4.7	6.5	5.6	1.3
M2(y)	3.1	4.3	3.7	0.9
M2 (z)	3.6	6.1	4.8	1.8
M3 (x)	7.6	7.5	7.6	0.1
M3 (y)	10.8	9.7	10.0	0.8
M3 (z)	7.4	6.7	7.1	0.5
M4 (x)	8.6	8.9	8.8	0.2
M4 (y)	8.6	9.5	9.1	0.6
M4 (z)	6.1	7.5	6.8	1.0
Average			6.4	0.8

Table 4.1: The linearity correction factors and residual linearity errors.

5

System verification and validation

Research question 2 reads, "What verification and validation procedures are suitable to test whether the magnetic measurement system fulfills the research objective?". The verification is conducted to check the systems performance against the written requirements of Chapter 2. The functional validation is conducted to check whether the system is able to do what it was designed for, measuring the field of a DUT. The verification is discussed in Section 5.1, the functional validation is discussed in Section 5.2.

5.1. System verification

In this section, the systems performance will be tested against the written requirements. Each requirement will be tested in turn. For requirements which are not met, an explanation is given in addition to a recommendation for how to meet this requirement in the future. Most of the requirements can be tested in a simple manner, whereas the validation of requirement 3.2 calls for a more extensive test. The requirements which only call for a brief test are discussed in the list below. Requirement 3.2 is discussed in Subsection 5.1.1. Table 5.3 summarizes the verification.

Req. 1.1 **The system shall be able to measure the magnetic field produced by the DUT at different positions around and/or on the DUT.** The moveable magnetometers enable measurements at almost all positions within the measurement system.

Req. 1.1.1 **The measurement system shall be able to produce a graph of the magnetic field over time on the positions where the field was measured.** The raw and calibrated measurement data is part of the output of the measurement system, along with a time indexing array. Thereby a graph of the magnetic field at the magnetometer locations can be produced.

Req. 1.2 **No magnetic materials shall be used in the supporting structure of the measurement system.** The supporting structure is entirely made out of PLA, which is has no magnetic properties.

Req. 1.3 **The measurement system shall be used in a magnetically clean environment.** Whether or not this requirement is met depends on the user.

Req. 1.4 **The target range for the cost of the magnetic field measurement system is 500 to 1500 Euros.** The magnetometers have a total cost of 302 Euros. The remaining components, including the Raspberry Pi Pico, breadboards, wires, USB cable and soldering headers have a cost of approximately 40 Euros. The total system cost is thus well below the minimal target cost.

Req. 2.1 **The supporting structure shall be able to hold DUTs ranging from a 3P PocketQube (192x71,6x70 mm (uncertainty ± 0,1 mm)), to an individual subsystem (50x50xh mm), in place.** The inside of the measurement system is an open space of 95x95x250 mm. This is large enough for a 3P PocketQube. If a smaller DUT is to be used, the height of the system can be halved. Furthermore thicker magnetometer holders can be used to place the magnetometers closer to the DUT. The system is thus usable for different sizes of DUTs.

Req. 2.2 **The measurement system shall have movable (by the user) magnetometers.** The magnetometers can be moved horizontally by using the rails, and by changing the thickness of the magnetometer holders. In the vertical direction, the magetometers can be placed into different rails or the DUT can be elevated using the 1 mm thin plates. As the vertical position of all magnetometers is changed when the DUT is elevated, the spatial resolution in the vertical direction of individual magnetometers is limited.

Req. 2.2.1 **The moving range of the movable magnetometers shall be** 212 mm **regarding the height, and** 91.6 mm **regarding the width and depth of the measurement system.** In the horizontal direction, the magnetometers can move in a rails of 95 mm. Considering the magnetometer dimensions, this means that the *center* of the magnetometer (where the sensors are located) can only move 70 mm. Requirement 2.2.1 is thus not met when it comes to the horizontal direction. The reason for this is that the walls of the 3D supporting structure were printed when a smaller magnetometer was being used. Redesigning the walls to be 21.6 mm longer solves this issue.
For the vertical direction, the magnetometers can be moved by changing the rails they are placed in, or by elevating the DUT. The former can only be done in increments of 1 rails separation, i.e. 38 mm. Elevation of the DUT allows for finer positioning, as the thin plates used for elevation are 1 mm thick. Elevation of the DUT causes a change in position for all magnetometers, thus one magnetometer can move freely over the entire height of the measurement system, whereas the other magnetometers have a fixed amount of DUT elevation, and can only be moved freely with increments of 38 mm. Requirement 2.2.1 is thus not met in the vertical direction.

Req. 2.3 **The supporting structure shall keep magnetometers in place at different positions.** As discussed, the magnetometers can move in all three directions. The magnetometer holders keep the magnetometers fixed in place during measurements. The magnetometer holders, in turn, are kept in place using the distance holders shown in Figure A.11. To keep the magnetometers in place at different positions around the DUT, different size distance holders can be used.

Req. 2.3.1 **The measurement system shall provide information regarding the positions of the magnetometers which can directly be entered into data analysis software.** For each magnetometer, the number of the used rails, the thickness of the magnetometer holder and the length of the distance holder used are given as input to the data processing software. Just as the amount of 1 mm thin plates used. From this information, the software can determine the position of each magnetometer.

Req. 2.4 **The system shall be usable without having to risk damaging the DUT.** For the largest DUT dimension, that of a 3P PocketQube, there is atleast 9 mm of additional open space on each side of the DUT. This is enough room to place the DUT in the measurement system and take it out, without the risk of damaging the DUT.

Req. 2.6 **The supporting structure shall facilitate magnetometer placement w.r.t. the DUT with an accuracy of** 2 mm**.** Placement of the DUT is done with an accuracy of 0.2 mm. Placement of the magnetometers is done with an accuracy of twice 0.2 mm. So the magnetometer placement w.r.t. the DUT has an error of 0.6 mm at most.

Req. 2.6.1 **The supporting structure shall facilitate placement of the DUT at the desired location w.r.t the supporting structure with an accuracy of** 1 mm**.** The DUT is to be placed in the middle of the measurement system. Depending on the dimensions of the bottom of the DUT, distance holders can be printed to keep the DUT in place w.r.t. the supporting structure. The printer tolerances of the 3D printer used are 0.2 mm, using a caliper it is confirmed that printed distance holders indeed fall within this tolerance. So the usage of distance holders for the DUT ensures the required accuracy is achieved.

Req. 2.6.2 **The supporting structure shall facilitate magnetometer placement on the supporting structure itself with an accuracy of** 1 mm**.** In the horizontal direction, the magnetometers are kept in place by the magnetometer holders and distance holders. The printer tolerances are 0.2 mm, thus meeting the requirement in the horizontal direction.
In the vertical direction the magnetometers can be moved between different rails individually, and thin plates can be used to elevate the DUT if a finer positioning is desired. The printer tolerances are 0.2 mm, which can occur both in the thin plates and in the horizontal wall. Thus an error of

0.2 mm times the amount of thin plates, plus 0.2 mm for the horizontal wall is possible. But if one uses a caliper to check the elevation due to the thin plates, it is always possible to add or remove one due to printer tolerance errors. Therefore it should always be possible to keep the vertical error below 1 mm. Note, this requirement is regarding accuracy, not spatial resolution.

Req. 2.7 **The supporting structure shall facilitate measurements on all sides of the DUT.** The bottom and top plates, as well as all horizontal walls of the measurement system feature multiple rails, in which magnetometers can be placed. The measurement system thus facilitates measurements on all sides of the DUT. A potential problem that is foreseen is that one might desire to conduct measurements on a DUT which needs to be exposed to sunlight (e.g. for solar panels). This requires one of the horizontal walls to be omitted, and thus means that no magnetometers can be placed on this side of the DUT. This can in turn be solved by designing a horizontal wall with as much open surface area as possible, such that it can support the magnetometers, but does not limit the exposure of the DUT to sunlight too much. This has not been done in the current design, but is an option to be pursued if one desires to conduct such measurements.

Req. 3.1 **The magnetometers shall be able to measure the magnitude and direction of the magnetic field.** The magnetometers used in the measurement system are the RM3100 developed by PNI sensor corporation. These are triaxial magneto-inductive magnetometers, which are capable of measuring both the magnetic field magnitude and direction.

Req. 3.2 **The cumulative error in magnetometer measurements shall be below** 34 nT **for each axis. The cumulative error is introduced by; the magnetometer residual linearity error, temperature drifts, magnetometer interference and magnetometer precision.** This requirement is discussed in Section 5.1.1.

Req. 3.3 **Magnetometers can be placed within** 50 mm **from one another.** In the horizontal direction, two magnetometers can be placed directly next to one another, save for the 2.1 mm thickness of the magnetometer holder in this dimension. So the magnetometers have a distance of 4.2 mm between them, and the sensors (which are in the center of the magnetometer) have a distance of 29.6 mm between them. Thus, in the horizontal direction requirement 3.3 is met.
In the vertical direction, the closest two sensors can be to one another is by one being one rails above the other, creating a distance of 38 mm between them. Thus in the vertical direction requirement 3.3 is also met.
As the vertical and horizontal locations of the magnetometers can be adjusted independently, requirement 3.3 as a whole is met.

Req. 3.4 **The magnetometers shall be operational in the magnetic field range of [-10, 10] μT if the EMF is nulled, and in the magnetic field range of [-55, 55] μT if the EMF is present.** The RM3100 has an operational range of [-800, 800] μT, thus meeting requirement 3.4.

Req. 3.5 **The magnetometer shall be able to measure with a measurement frequency of** 150 Hz**.** The RM3100 conducts a measurement based on the time it takes a positive and negative current to pass the oscillator. The amount of oscillations per measurement is called the cycle count, and is user configurable. A high cycle count improves the magnetometer resolution, but reduces the measurement frequency. The magnetometers are operated using a cycle count of 200, which is recommended if a high resolution is desired. This limits the maximum measurement frequency of a single magnetometer measuring in three directions to 146 Hz. To meet requirement 3.5, the cycle count can be lowered, thereby increasing the measurement frequency but lowering the resolution. This is not done currently, as a magnetometer setting which optimizes resolution is favoured.

Req. 4.1 **An independent user needs to be able to operate the data acquisition software, without additional help from the author.**

Req. 4.1.1 **The software needed for data acquisition shall be commented in such a manner that the function of each line of code is transparent for an independent user.** The software is well documented, the purpose of each line of code is clear. However, it is impossible to validate this requirement fully at this stage, as this would require a different user to read the user manual and familiarize themselves with magnetic measurements.

Req. 4.1.2 **In the software needed for data acquisition a clear distinction shall be present between what settings a user is supposed to change, depending on their preferences, and what settings are supposed to be left unchanged.** User configurable settings are grouped together, and comments clearly indicate which settings to change, and which to leave unchanged. However, it is impossible to validate this requirement fully at this stage, as this would require a different user to read the user manual and familiarize themselves with magnetic measurements.

Req. 4.2 **The output of the data acquisition software shall be a .csv or .dat file OR the data shall be exported live to a different software. One of these two methods will suffice.** The data is exported live to a different software (Matlab), where it is stored as a data file.

Req. 4.3 **The digital resolution of the data acquisition subsystem should be below** 17 nT **(i.e. 17 nT/LSB or 59 LSB/µT).** A single measurement in a single direction is saved as a 24 bit value in the data acquisition subsystem. The least significant bit (LSB) has a value of 13.3 nT, thus meeting requirement 4.3.

Req. 4.4 **The baud rate of the micro controller shall be** 400 kHz**.** The fast mode of the Raspberry Pi Pico is used, which is 400 kHz.

Req. 4.5 **The data acquisition software shall need no longer than** 6.6 ms **total to read one measurement from all magnetometers.** The data acquisition software loop which reads the measurements from all magnetometers takes 4 ms, thus meeting requirement 4.5.

Req. 4.6 **The magnetometer data will be read using a data ready signal.**

Req. 4.6.1 **The data ready pins shall be checked by the microcontroller with a frequency of atleast** 1 MHz**.** The microcontroller checks whether the data pins are ready with a frequency of 6.2 MHz, thus meeting requirement 4.6.1.

Req. 4.6.2 **A positive data ready signal shall be read by the microcontroller for each magnetometer, before the data of all magnetometers is read.** The microcontroller only starts reading measurement data once all data ready pins provide a positive data ready signal.

Req. 4.6.3 **Each magnetometer shall give a data ready signal on a designated data ready pin when a measurement is conducted, which can be read by the microcontroller.** A separate data ready pin is assigned to each magnetometer, as shown in Figure 3.8.

Req. 4.7 **An independent user needs to be able to operate the data processing software, without additional help from the author.** The software is well documented, the purpose of each line of code is clear. User configurable settings are grouped together, and comments clearly indicate which settings to change, and which to leave unchanged. However, it is impossible to validate this requirement fully at this stage, as this would require a different user to read the user manual and familiarize themselves with magnetic measurements.

Req. 4.8 **The measurement duration shall be changeable by the user.** The measurement duration can be changed in the data readout script Data_reader_4sensors.m.

Req. 4.9 **The output of data processing will contain the following elements:**

- The raw measurement data in each direction.
- Average measured magnetic field of the DUT in each direction.
- Standard deviation of the average measured magnetic field.
- Kurtosis of the average measured magnetic field.
- Maximum and minimum values of the measured magnetic field.
- Maximum and minimum values of the measured magnetic field corresponding to a 99.7% confidence interval.
- Fourier transform of the measured data ranging from 0 Hz to 75 Hz.
- The PSD and autocorrelation of the measured noise, both graphically displayed.
- The lag value for which the autocorrelation of the measured noise drops below 0.1

In Section 3.3.2 the output as provided by the data processing software is explained. The figures will not be repeated in this chapter. The table shown in Figure 3.10 contains all the required output as listed in requirement 4.9, apart from the output which is to be displayed graphically. Figures 3.13, 3.14 and 3.15 show the Fourier transform, PSD and autocorrelation of a sample measurement. Due to requirement 3.5, regarding the measurement frequency, not being met, the Fourier transform has a smaller range than specified in requirement 4.9. On all other aspects, requirement 4.9 is met.

Req. 4.10 **Output will be separated by magnetometer locations.** The output shown in Figures 3.10 to 3.15 is all related to Magnetometer 1, similar outputs are available for M2, M3 and M4. The magnetometer locations relative to the DUT are graphically displayed as shown in Figures 3.11 and 3.12.

Req. 4.11 **Output will be separated in the x-, y- and z-direction, as well as a total value.** It can be seen in Figures 3.10 and 3.13 to 3.15 that the output is separated in the x-, y- and z-direction, a total value is included where it is relevant.

5.1.1. Verification of requirement 3.2

Requirement 3.2 reads: "The cumulative error in magnetometer measurements shall be below 34 nT for each axis. The cumulative error is introduced by; the magnetometer residual linearity error, temperature drifts, magnetometer interference and magnetometer precision."
In this section the contribution of the four error factors will be discussed in turn, with a conclusion on the total error being presented at the end of the section.

Magnetometer precision

Magnetometer precision defines how closely repeated measurements of the same magnetic field are grouped together, as illustrated in Figure 2.2. The magnetometer precision is quantified by the spread in measurements on a constant magnetic field. Without an environment which actively nulls the EMF and, more importantly, its fluctuations, it is impossible to distinguish which contribution in the spread of measurements is due to magnetometer precision, and due to noise. Therefore the error due to environmental noise will be included in the magnetometer precision error.
To minimize the error due to magnetometer precision and surrounding noise, multiple measurements are conducted in quick succession, the average of which is taken. The uncertainty of this average value is the standard deviation of the mean, as defined in Equation 2.1.
To quantify the error, multiple tests have been conducted over the course of a few days, with each test being an average over 200 measurements. The standard deviation of the mean for these test varies between 5 nT and 9 nT for each axis, these tests were conducted both in the Plasma Laboratory at Eindhoven University of Technology and the Cleanroom of the Aerospace faculty at Delft University of Technology. It should be noted that in a different environment, or a different moment in time, more or stronger noise sources might be present, so it is recommended to test for noise sources before using the measurement system. This can be done as described above.
The error due to magnetometer precision and noise, which is 9 nT for each axis, is *below* the RM3100 resolution, which has a value of 13 nT. This is an effect of using the standard deviation of the mean to quantify the error in the *average* measured magnetic field.

Residual linearity error

The linearity error has been corrected for using a correction factor as described in the calibration procedure in Chapter 4. The standard deviation in the correction factors determined during different measurements on the same magnetometer axis quantifies the residual linearity error for said axis.
The residual linearity errors have already been presented in Table 4.1, but are for convenience repeated in Table 5.1. The second column in Table 5.1 shows that the residual linearity error differs for each magnetometer and for each axis. This is largely attributed to the shortcomings of the calibration procedure, as described in Section 4.2. The residual linearity error averages 0.8%. Thus, an average error of 8 nT can be expected in the measurements per μT of DUT magnetic field.

Temperature drift

PNI sensor corporation claims that RM3100 measurements are stable for different temperatures within its operational temperature range ([-45, 80 ° C]) [3]. To validate this, the magnetometers are placed in a constant

Magnetometer (axis)	Residual linearity error [%]
M1 (x)	0.7
M1 (y)	0.4
M1 (z)	1.3
M2(x)	1.3
M2(y)	0.9
M2 (z)	1.8
M3 (x)	0.1
M3 (y)	0.8
M3 (z)	0.5
M4 (x)	0.2
M4 (y)	0.6
M4 (z)	1.0
Average	0.8

Table 5.1: The residual linearity error for each magnetometer axis.

magnetic field and measurements are conducted for different magnetometer temperatures. If the magnetometers are indeed stable for different temperatures, the magnetic field measurements for different temperatures should lie on a horizontal line, or within a standard deviation above or below it.
Figure 5.1 shows the magnetic field measurements of M1 for different temperatures. On the vertical axis, the change in magnetic field w.r.t. the first measurement point (20.8 ° C) is shown. Each measurement point is obtained by taking the average over 213 consecutive measurements (at a frequency of 37 Hz), and has an error of approximately $\sigma_m = 6$ nT (not shown). It can be observed that no upward or downward drift is present for any of the axes, but it is clear that the measured magnetic field deviates from a constant horizontal line by more than the expected amount. This is attributed to small magnetic field fluctuations and variations in the laboratory during the heating of the magnetometers, as this took quite some time (about 10 minutes).
As no drift is observed with changing temperature, the claim from PNI sensor corporation is likely true, and no error due to temperature changes will be taken into account.

Magnetometer interference
To test whether magnetometer interference causes an error, the measurement system is placed in a constant magnetic field. Magnetometers 1 and 2 are placed in the same rails of the measurement system. A measurements lasting 20 s is conducted, over the course of the measurement magnetometer 2 is moved closer to, and farther away from, magnetometer 1 twice. This is shown as the orange line in Figure 5.2. It should be noted that the moving of magnetometer 2 was done by hand, so it did not happen precisely as shown in Figure 5.2.
The blue line in Figure 5.2 shows the measured magnetic field of M1 in all three axes, with a moving average filter of 15. As no correlation between the magnetometer separation and the measured magnetic field is observed in Figure 5.2, it is concluded that magnetometer interference does not add an error to the measurements.
The lack of influence due to magnetometer interference is attributed to the fact that the magnetic sensors are on a breakout board with a size of 25.4 mm and are held in place by a magnetometer holder. The sensors themselves are thus not right next to one another when the magnetometer holders are moved right next to one another.

Total magnetometer uncertainty
The total magnetometer uncertainty can be found by summing the different errors described above. The different uncertainty contributions are listed in Table 5.2. The total uncertainty shown in Table 5.2 is for a DUT magnetic field of 10 µT, as per requirement 3.4. For smaller DUT magnetic fields, the total uncertainty can be estimated using

$$\sigma_{tot} = 9 + 8.0 B_{DUT}, \tag{5.1}$$

where σ_{tot} is the total uncertainty in nT and B_{DUT} the DUT magnetic field in µT.

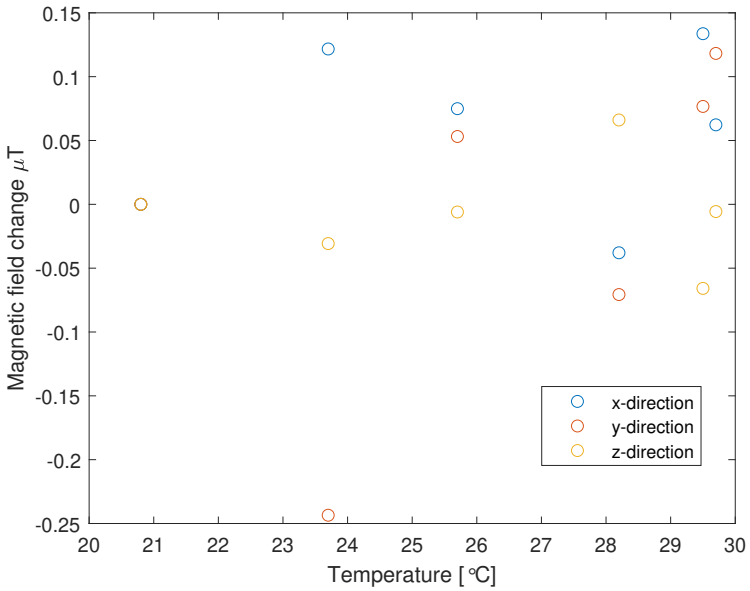

Figure 5.1: The change in magnetic field as a function of temperature, for M1. Note that the leftmost data point overlaps for all 3 directions.

Uncertainty contribution	**Error** [nT]
Magnetometer precision and noise	9
Residual linearity error	80
Temperature drift	-
Magnetometer interference	-
Total uncertainty (σ_{tot})	80.5

Table 5.2: The magnetometer uncertainty and different contributions, assuming a DUT magnetic field of 10 µT .

Equation 5.1 shows that requirement 3.2 is not met for the full range of DUT magnetic fields. If the DUT magnetic field is 3.1 µT or smaller along a specific axis, the total uncertainty for said axis remains within the required uncertainty margin of 34 nT.
To meet requirement 3.2 for the entire range of DUT magnetic fields, the residual linearity error must be decreased. This can be done following the recommendations described in Section 4.2.

5.1.2. Summary of the system verification

The purpose of the system verification is to test whether the measurement system meets the system requirements as defined in Chapter 2. Table 5.3 summarizes which requirements are met, which are not met, and which are partially met or require independent user verification. The failed requirements are related to the horizontal moving range and vertical spatial resolution of the magnetometers (Req. 2.2) and the magnetometer measurement frequency (Req. 3.5). The most important requirement which is only partially met is related to the magnetometer measurement uncertainty (Req. 3.2). The uncertainty of the measurement system is only below 34 nT for DUT magnetic fields below 3.1 µT along a specific axis, which is less that the entire operational range of the measurement system should be as defined in requirement 3.4.

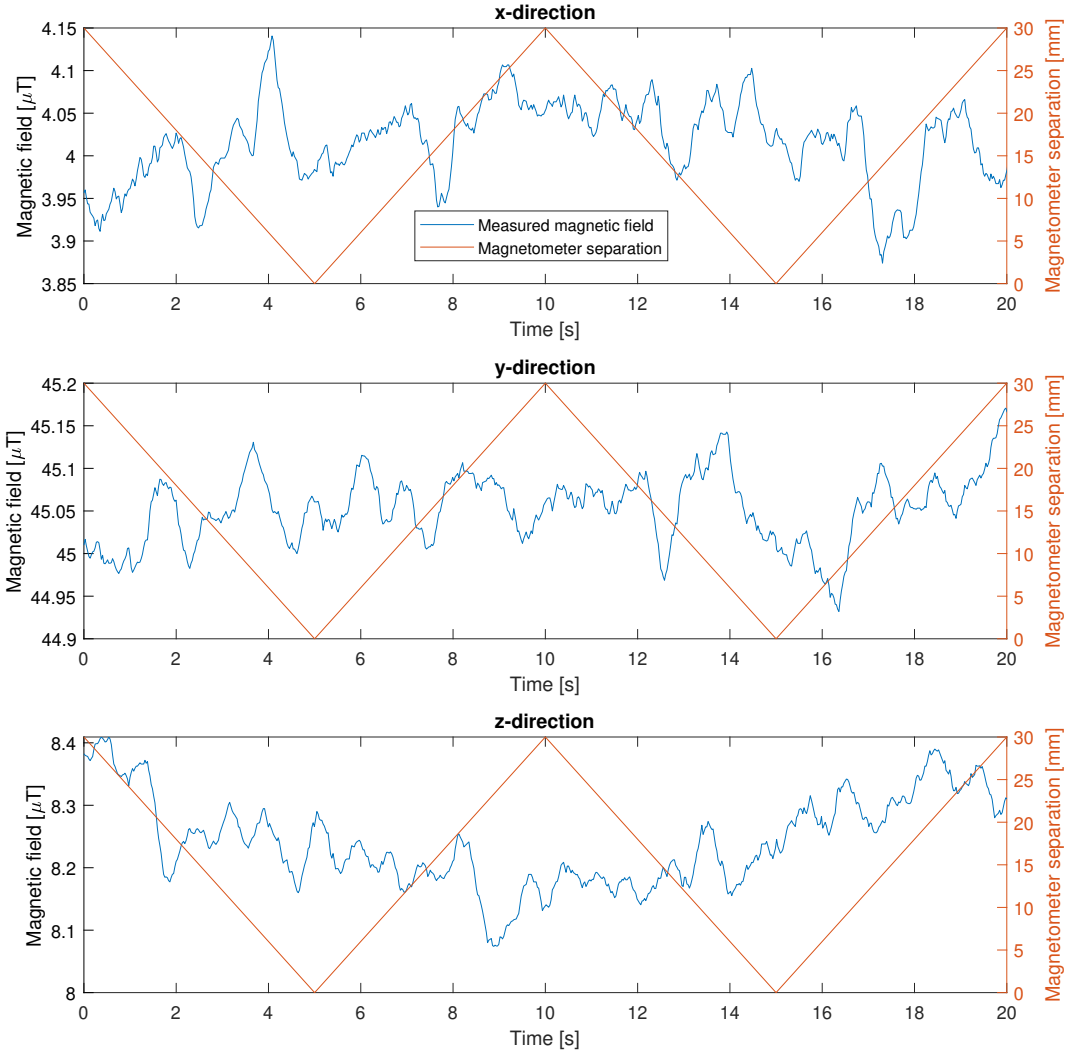

Figure 5.2: Magnetic field measurements for a changing magnetometer separation.

Requirement	Verification	Comment
1.1	Check	
1.1.1	Check	
1.2	Check	
1.3	Depends on user chosen location.	
1.4	Check	
2.1	Check	
2.2	Fail	
2.2.1	Fail	Horizontal range too short. Vertical spatial resolution too low
2.3	Check	
2.3.1	Check	
2.4	Check	
2.6	Check	
2.6.1	Check	
2.6.2	Check	
2.7	Check	
3.1	Check	
3.2	Only up to DUT fields of 2.4 µT.	Improve calibration, separate magnetometers.
3.3	Check	
3.4	Check	
3.5	Fail	Resolution is currently favoured over frequency.
4.1	Check	Needs independent user verification
4.1.1	Check	Needs independent user verification
4.1.2	Check	Needs independent user verification
4.2	Check	
4.3	Check	
4.4	Check	
4.5	Check	
4.6	Check	
4.6.1	Check	
4.6.2	Check	
4.6.3	Check	
4.7	Check	Needs independent user verification
4.8	Check	
4.9	Fourier transform limited range	Due to requirement 3.5 not being met, the range of the Fourier transform is less than required.
4.10	Check	
4.11	Check	

Table 5.3: Requirements checklist.

5.2. Functional validation

The functional validation serves to test whether the measurement system fulfills its purpose, which is stated in the research objective.

To develop a measurement system which is capable of characterizing the satellite magnetic fields of small satellites close to the satellite body itself.

In the verification is has been shown that the uncertainty of the measurement system is higher than 34 nT per axis for DUT fields above 3.1 µT, so the research objective is not achieved in this regard. The goal of the functional validation is to test whether the measurement system functions as intended besides the uncertainty. The methodology of the functional validation is described in Subsection 5.2.1. Subsection 5.2.2 will discuss the results of these tests and Subsection 5.2.3 will discuss the conclusions which can be drawn from said results and how the system can be used for the improvement of pointing accuracy.

5.2.1. Functional validation methodology

The functional validation will consist of different measurements with different purposes. The different measurements will be explained below. All measurements will be conducted using Delfi-PQ as DUT.

- By conducting a background measurement, a measurement with Delfi switched on (ON) and a measurement with Delfi switched off (OFF), the average DUT magnetic field is investigated. By subtracting the background measurement from the OFF measurement, the passive magnetic field of Delfi is found. By subtracting the OFF measurement from the ON measurement, the active field of Delfi is found. As the background, OFF and ON measurements are conducted at different moments in time, one cannot subtract the calibrated data from one another directly. Rather, the average background, OFF and ON magnetic field is calculated for each axis separately. It are these average values which are subtracted from one another. This holds for all measurements in the functional validation, unless specified otherwise. The background-OFF-ON measurement cycle is repeated five times. The average of DUT ON and OFF measured magnetic field over these five cycles will be taken. It should be noted that for any measurement with Delfi-PQ being switched ON, it is ensured that the measurement is conducted between data transmissions, as to not disrupt the measurement. For this measurement two magnetometers will be placed close to the battery pack, one will be placed near the bottom of Delfi, and one will be placed in the middle of Delfi. This magnetometer configuration is shown in Figures 5.3 and 5.4.
- To investigate the effect of the antennae being folded or deployed, the above measurements are done once for the folded state, and once for the deployed state.
- A background-OFF-ON measurement cycle as described above will be conducted using a different magnetometer configuration. For this measurement, the magnetometers will all be placed close to the battery pack. They will have the same z-coordinate, but will be placed at different x-,and y-coordinates. This magnetometer configuration is shown in Figures 5.5 and 5.6. The purpose of this measurement is to investigate whether the DUT magnetic field is rotationally symmetric in the z-axis around the battery pack.
- A background-OFF-ON measurement cycle as described above will be conducted using a different magnetometer configuration. For this measurement, the magnetometers will all be placed on the same x-, and y-coordinates, while having different z-coordinates. This magnetometer configuration is shown in Figures 5.7 and 5.8. The purpose of this measurement is to investigate how the DUT magnetic field changes with height.
- To investigate dynamic effects, a measurement (in the deployed configuration) lasting for 110 s will be conducted. For this measurement, the average background magnetic field will be subtracted from the calibrated data, to preserve the dynamic effects (rather than averaging over the measurement). The Fourier spectrum of this measurement should reveal a peak for the data transmission of the antennae, which happens once every minute. The measurement is started such that two data transmissions fall within the measurement. The magnetometer configuration for this measurement will be the same as the first measurement, as shown in Figures 5.3 and 5.4.

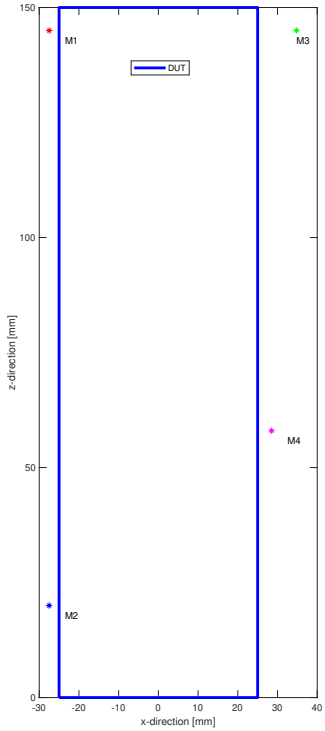

Figure 5.3: Topview of the magnetometer locations around the DUT for configuration 1 (axes in mm).

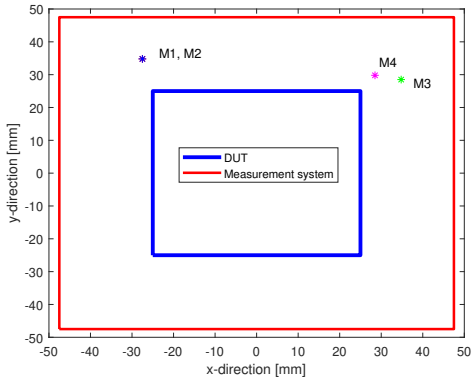

Figure 5.4: Sideview of the magnetometer locations around the DUT for configuration 1 (axes in mm).

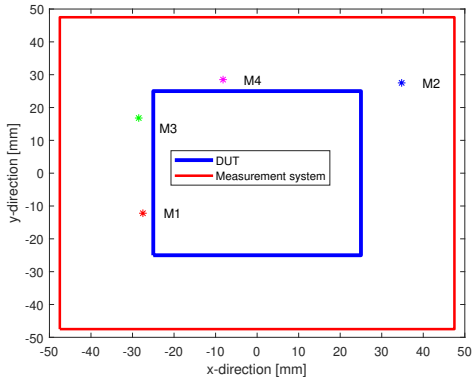

Figure 5.5: Topview of the magnetometer locations around the DUT for configuration 2.

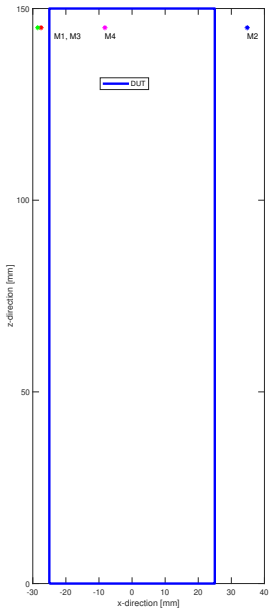

Figure 5.6: Sideview of the magnetometer locations around the DUT for configuration 2.

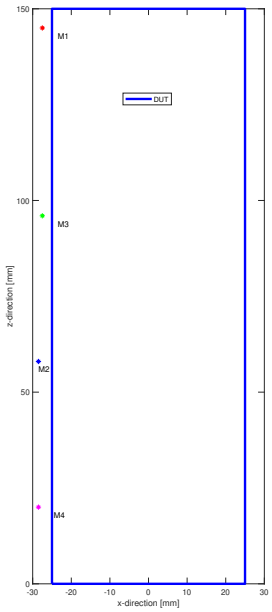

Figure 5.7: Topview of the magnetometer locations around the DUT for configuration 3.

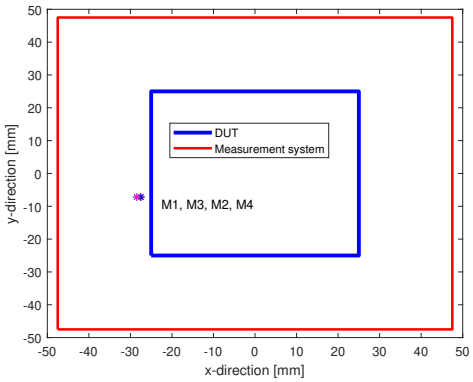

Figure 5.8: Sideview of the magnetometer locations around the DUT for configuration 3.

5.2.2. Functional validation results

In this subsection the results of the different functional validation measurements will be discussed. The results will be discussed per measurement.

Configuration 1

The first measurements concerns a spread of magnetometers, as shown in Figures 5.3 and 5.4, and is conducted as described in Subsection 5.2.1. Table 5.4 shows the resulting measured magnetic field for both the folded and deployed states of Delfi-PQ, both with the satellite being switched ON and OFF. The difference in measured magnetic field between Delfi being switched ON and OFF is small, and mostly falls within the standard deviation denoted in Table 5.4. Thus, for this configuration only a passive field is measured.
A difference between the magnetic fields for the deployed and folded configuration is observed for M2 and M3, while M1 and M4 show no significant change. The difference for M3 could potentially be explained by the fact that it is quite close to the antenna in the folded state of Delfi, whereas it is far away from the antenna in the deployed state. The same is however expected for M1, whereas this is not expected for M2, thus there is likely another reason for the difference in the magnetic fields measured by M2 and M3.

Configuration 2

Configuration 2 concerns measurements with all magnetometers being placed around the battery pack, as shown in Figures 5.5 and 5.6, and is conducted as described in Subsection 5.2.1. Table 5.4 shows the results of the measurements. For this magnetometer configuration a clear difference in magnetic field between Delfi being ON and OFF is observed. This difference is largest for M1, and smallest for M2, which is likely due to them being the closest and furthest from the battery pack, respectively. In close proximity to the battery pack, the active magnetic field of Delfi-PQ can thus be clearly distinguished from the passive field.
From Figure 5.5 it can be seen that M1 and M4 face different sides of Delfi-PQ. Their position w.r.t. these faces are almost identical, the difference being that M4 is 4 mm closer to the center of Delfi's side than M1. The magnetic field measured by M1 is 3.6 ± 0.2 µT and 5.5 ± 0.1 µT for Delfi being ON and OFF respectively (here σ_m is used to quantify the uncertainty). The magnetic field measured by M4 is 2.3 ± 0.2 µT and 3.4 ± 0.3 µT for Delfi being ON and OFF respectively. The large difference between the magnetic field at the locations of M1 and M4 indicates that the magnetic field produced by the battery pack is not rotationally symmetric.

Configuration 3
Configuration 3 concerns measurements with all magnetometers being placed in a vertical line, as shown in Figures 5.7 and 5.8, and is conducted as described in Subsection 5.2.1. The results are shown in Table 5.4, it should be noted that the magnetometers are *not* placed in order in Figure 5.7. From Table 5.4 it is observed that the magnetic field of Delfi is the strongest at the top of Delfi, and weakest at the bottom. But it is also observed that the magnetic field does not decrease monotonically, as M2 measures a larger field than M3. This indicates that there is/are (an)other magnetic field source(s) present in Delfi below the battery pack. Whether the source is close to M2 or M3 cannot be concluded from this measurement, as any source can have a positive or negative contribution to the total measured magnetic field.

Dynamic measurement
To investigate dynamic effects, a measurement lasting 110 s is conducted, as described in Subsection 5.2.1. The magnetometers are placed in configuration 1, as shown in Figures 5.3 and 5.4. Delfi-PQ is switched ON for this measurement, and is in its deployed state. Figure 5.9 shows the calibrated measurement data, which has been corrected for the background magnetic field. Clear peaks are observed for M1 and M3, at a frequency of 1 minute, which is the frequency of data transmission from Delfi-PQ. No such peaks are observed for M2 and M4. The peaks observed for M1 and M3, which are close to the battery pack, are attributed to the communications subsystem drawing a large current from the battery during data transmission. This causes a magnetic field change at the location of the battery pack during transmission. As the antennae transmit data at a frequency far above the measurement frequency of the magnetometers, it is not expected that any peaks are observed for M2 and M4, which are farther from the battery and closer to the antennae. The dynamic effects from the data transmission can thus be measured in close proximity to the battery pack.
It can be seen that M1 and M3 measure the transmission peaks for different axes. This is explained by the fact that M1 is mounted on the left wall shown in Figure 5.4, whereas M3 is mounted on the upper wall in Figure 5.4. This means that the magnetometers have a different orientation. The x-axis of M1 points in the same direction as the *negative* z-axis of M3. The y-axis has the same orientation for M1 and M3, while the measured transmission peak is much more prominent for M3. Figure 5.10 shows the normalized Fourier transform of the above described measurement. The Fourier transform has been normalized to the DC amplitude, and has been cut off at 1 Hz. This has been done as the DC frequency dominates, as can be seen on the vertical axis of Figure 5.10. It can be observed from Figure 5.10 that no frequencies above 1 Hz have a contribution of more than 0.1% to the magnetic field of Delfi-PQ. For any frequency above half the measurement frequency, no conclusion can be drawn. The expected peak due to the data transmission could not be distinguished from the DC peak.

Delfi-PQ conclusions
Here a short summary of the conclusions found from the measurements on Delfi-PQ with the magnetic measurement system will be given. The conclusions will be presented as a list.

- The passive field of Delfi-PQ has been measured for different magnetometer configurations. The field is largest close to the battery pack. Other magnetic field source(s) have been observed.
- Delfi-PQ produces an active magnetic field which is observed close to the battery pack. Farther away from the battery pack no change in magnetic field is observed when Delfi is switched ON or OFF.
- The magnetic field around the battery pack does not appear to be rotationally symmetric.
- During data transmission the communications subsystem draws a large current from the battery pack. This gives rise to a magnetic field change close to the battery pack which is observed. Delfi-PQ does not have magnetic sources producing a magnetic field with a strength of more than 0.1% of the DC field in the range of 1 Hz to 18 Hz.
- Besides the battery pack, another magnetic field source is measured in configuration 2.

5.2.3. Functional validation of the system
The purpose of the functional validation is to investigate to what degree the measurement system can fulfill the research objective. During the functional validation the measurement system has successfully measured

Measurement	Parameter	M1 (ON)	M2	M3	M4	M1 (OFF)	M2	M3	M4
Config 1, folded	Average [μT]	2,54	1,39	1,71	0,52	2,50	1,30	1,89	0,55
	St. dev. [μT]	0,12	0,03	0,14	0,12	0,07	0,19	0,15	0,12
Config 1, deployed	Average [μT]	2,63	0,23	0,84	0,54	2,60	0,21	0,99	0,47
	St. dev [μT]	0,21	0,10	0,17	0,18	0,15	0,04	0,15	0,13
Config 2	Average [μT]	3,64	0,36	1,84	2,33	5,46	0,70	2,69	3,44
	St. dev. [μT]	0,37	0,17	0,10	0,44	0,12	0,33	0,25	0,47
Config 3	Average [μT]	6,19	1,33	1,08	0,66	6,04	1,34	1,04	0,60
	St. dev. [μT]	0,54	0,37	0,34	0,13	0,33	0,39	0,29	0,17

Table 5.4: Results from the functional validation measurements.

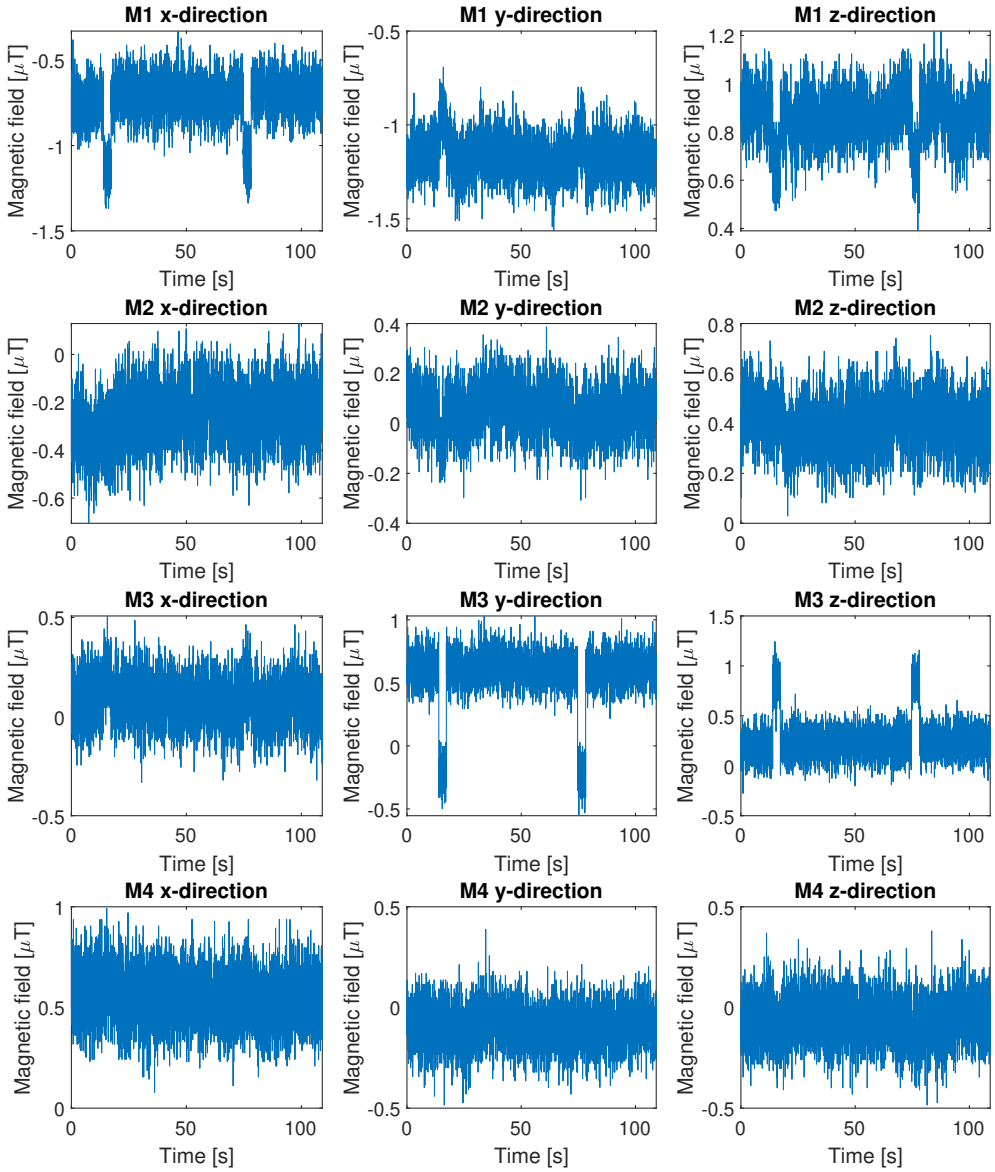

Figure 5.9: Results of the measurement investigating dynamics.

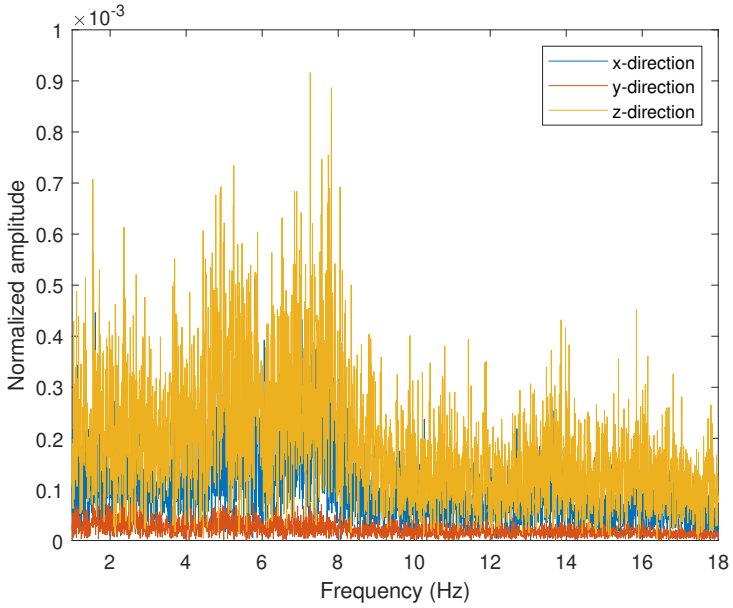

Figure 5.10: The normalized Fourier transform of a measurement on Delfi-PQ as it was ON, cut off at 1 Hz.

both the passive and active magnetic field of Delfi-PQ. The magnetic field has been measured at different locations around the satellite. The measurement system is modular, and changes between different magnetometer configurations were easily applied and implemented in the data acquisition and processing software. The data acquisition and processing software allowed for quick data analysis right after the measurements were conducted. The measurement system is able to measure dynamic effects in the magnetic field of Delfi-PQ up to 18 Hz.
Apart from this, some flaws in the measurement system have been observed during the functional validation, which prevent it from fulfilling the research objective with respect to some requirements. These flaws are listed below.

- The repeatability error of the measurement system is quantified as the standard deviation *of the mean* for multiple measurements. For the total measured magnetic field in configuration 1, this is typically between 0.08 µT and 0.1 µT. This is larger than the sum of individual uncertainties found in Section 5.1.1. This is attributed to the fact that the measurement system was designed for Delfi being in its folded state, and not in its deployed state. This was fixed with a quick workaround, but resulted in the measurement system having to be lifted and placed back for each background-OFF-ON cycle. In doing so, it is likely that the positions of the magnetometers w.r.t. Delfi-PQ changed slightly. Even though this increases the uncertainty in the measurements, the measurement system is still capable of measuring the magnetic field of Delfi-PQ with a relative error below 10% when measuring in close proximity to the battery pack.
  To investigate whether the uncertainty of 0.1 µT could be due to environmental noise a background measurement lasting 20 s was conducted. The standard deviation of the mean in this measurement is 4 nT, which is well below the 0.1 µT repeatability error. This repeatability error is thus not caused by environmental noise.

- When the measurement system is lifted and placed back, the position of the magnetometer is changed slightly, but so is its orientation. The change in orientation does not change the total magnetic field which the magnetometer measures, but it does change the measurements of individual axes. For this reason, it is not allowed to apply the central limit theorem on the measurement results for individual axes, and the standard deviation *of the mean* may not be used. This results in a repeatability error in configuration 1 between 0.05 µT and 0.2 µT for individual magnetometer axes. This uncertainty is, in most cases, higher than the uncertainty in the total measured magnetic field.

Direction	X [nT]	Y [nT]	Z [nT]	Inclination [Deg]	Declination [Deg]
Magnetic field	19155	709	45460	22.9	2.1
Uncertainty in EMF model	135	101	168	0.2	0.3
Uncertainty with calibrated magnetometer	241	224	261	0.3	0.7
Uncertainty with uncalibrated magnetometer	518	510	527	0.6	1.5

Table 5.5: Uncertainties in single axis measurements and point errors for a 'perfect', calibrated and uncalibrated magnetometer.

Calibrating ADCS magnetometers on Delfi-PQ
To investigate whether the measurement system can be used to calibrate ADCS magnetometers on CubeSats and PocketQubes, an example is worked out using measurements on the bottom of Delfi-PQ.
Current on board ADCS magnetometers are often placed on CubeSats and PocketQubes without measuring the satellite magnetic field. They are just placed as far away from the battery pack as possible [12]. Using the measurement system, the measurements of on board magnetometers can be corrected for the satellite magnetic field, with a remaining uncertainty of 0.2 µT per axis. For Delfi-PQ the measured field is 0.5 ± 0.2 µT per axis. Using this measurement for on board magnetometer calibration would remove the 0.5 µT measurement error of the on board magnetometer, whilst the 0.2 µT measurement uncertainty remains.
This results in an improved pointing accuracy for Delfi-PQ. Taking the EMF above Delft as an example, the pointing errors for a perfect magnetometer, a calibrated magnetometer and an uncalibrated magnetometer can be calculated. These magnetometers have uncertainties of 0 µT, 0.2 µT and 0.5 µT per axis respectively.
The magnetic inclination and declination of a satellite are calculated from the measured x-, y- and z-components of the magnetic field, and comparing these to an EMF model. For a perfect magnetometer, the only error would be from the uncertainty in the EMF model, shown in row 3 of Table 5.5. For a magnetometer exposed to the satellite magnetic field, the measurement uncertainty increases the total pointing error. Table 5.5 shows the uncertainties per axis and the resulting pointing errors for both an uncalibrated magnetometer at the bottom of Delfi-PQ, as well as a calibrated one. It can be seen that the error in magnetic inclination and declination is reduced from 0.6 and 1.5 degrees to 0.3 and 0.7 degrees respectively by calibrating the ADCS magnetometer. It should be noted that these numbers only account for uncertainties in the EMF model and due to the satellite magnetic field, but not due to any other factors.

This concludes the functional validation of the measurement system. It has been shown that the system can be used to characterize the satellite magnetic fields of small satellites close to the satellite body itself. Yet, the repeatability error of the measurement system is 0.1 µT, which is above the uncertainty as defined in the requirements. For separate axes, the repeatability error is 0.2 µT, due to the orientation of the magnetometers changing.

6

Conclusion

In this chapter a conclusion is drawn as to how well the research objective has been fulfilled. An answer to each of the research questions is formulated in Sections 6.1 to 6.3, followed by recommendations for future work in Section 6.4.

6.1. System capabilities

The research objective of this thesis project is;

To develop a measurement system which is capable of characterizing the satellite magnetic fields of small satellites close to the satellite body itself.

Research question 1 reads, "What applications will a measurement system for small satellites have and what capabilities should such a measurement system have?". The application of the magnetic measurement system is to measure the satellite magnetic field at various locations around the satellite. These measurements can then be used to select the most optimal position for an on board ADCS magnetometer and calibrate said ADCS magnetometer. One can use the Fourier spectrum of the measurement data to identify which components of the satellite contribute most to the satellite magnetic field. To fulfill the research objective and be useful with regards to these applications, the magnetic measurement system needs to be capable of measuring the magnetic field all around the satellite. The measurement system needs to be able to encompass DUTs ranging from a large 3U CubeSat, to a small subsystem of a CubeSat or PocketQube. To these ends, moveable magnetometers are needed, which can be positioned easily at the desired location w.r.t. the DUT. As the measurement system focuses on characterizing satellite magnetic field for the improvement of ADCS magnetometers, the system needs to be able to measure the DUT magnetic field with an uncertainty of 34 nT or lower. These capabilities have been formulated in engineering terms in the system requirements, discussed in Chapter 2.
To meet these requirements, a measurement system consisting of 3 subsystems has been designed and manufactured. The three subsystems are the magnetometers, the supporting structure and the data acquisition and processing software. To select the right magnetometer a parametric search was performed spanning five distributors of small electronics. Using criteria which followed from the requirements the RM3100 magnetometer was selected, mainly because it has a high resolution, low noise and low cost while meeting all other criteria on par with competitors. The supporting structure is designed using 3D modelling software, and is 3D printed from polylactic acid (PLA). The 3D printer used has tolerances of 0.2 mm, well below the required accuracy of 1 mm. The data acquisition and processing software is designed to enable measurements using different magnetometer settings in quick succession. As a whole, the system is designed to be modular, which allows for different DUTs and magnetometer configurations.

6.2. System tests

Research question 2 reads, "What verification and validation procedures are suitable to test whether the magnetic measurement system fulfills the research objective?".
The verification of the system checks the systems performance against the written requirements, and will be

discussed directly below. The validation checks whether the system meets the research objective, and will be discussed after the verification.

Verification
For each requirement, a method to test whether the requirement is met is discussed in Chapter 5.1. The verification shows that most requirements are met successfully, with a few exceptions listed below.

- Requirement 2.2.1, regarding the magnetometer mobility, is not met. In the horizontal direction, the moving range is 70 mm, instead of the required 91.6 mm. The limited horizontal moving range is not expected to be a significant issue, and is easily fixed by redesigning the walls. In the vertical direction the magnetometers have sufficient moving range, but they have a limited spatial resolution. In a single measurement vertical magnetometer separation can only be done with increments of 38 mm.
  So for a magnetometer configurations with vertical magnetometer positions which are not an integer times 38 mm apart, separate measurements per magnetometer need to be conducted. The effect of this is that the data of each magnetometer does not correspond to the same time-frame, and makes it impossible to observe dynamic effects with multiple magnetometers simultaneously. Solving this issue allows for a wider range of possible magnetometer configurations for the observation of dynamic effects.

- Requirement 3.2, regarding the measurement uncertainty, is not met. The uncertainty of the magnetometers is only below the required 34 nT for a DUT magnetic field of 3.1 µT or less, whereas the magnetometers should be able to handle DUT magnetic fields up to 10 µT.
  The effect of this requirement not being met is that the measurement system cannot measure DUT fields above 3.1 µT with the required accuracy. From the functional validation it was learned that for Delfi-PQ, a PocketQube produced by the TU Delft, the magnetic field within approximately 20 mm of the battery pack exceeds this value. Measurements around the remainder of Delfi-PQ resulted in magnetic fields below 3.1 µT. Thus the measurement system is not capable of producing accurate measurement results in close proximity to the battery pack. Due to the high magnetic field of the battery pack, it is not recommended to place ADCS magnetometers in its proximity. If one ensures that the magnetometers of the measurement system are also not placed within 20 mm of the battery pack, the system meets requirement 3.2 on all locations which are of interest for the purpose of improving ADCS magnetometers.

- Requirement 3.5, regarding the measurement frequency, is not met. At the moment the magnetometers have a measurement frequency of 37 Hz, instead of the required 150 Hz. This is due to the magnetometers being set to favour resolution over frequency.
  The effect of this requirement not being met is that dynamic effects of the magnetic field with a frequency above half the measurement frequency, thus 18 Hz, will not be observed in the measurements. To account for this, a setting with a higher measurement frequency can be selected. This will come with a lower resolution.

Apart from these requirements which are not met, the other requirements are met successfully. The measurement system is able to measure the magnetic field of the DUT at places all around the DUT (Req. 1.1). The user can place the magnetometers at desired positions with an accuracy below the required 2 mm (Req. 2.6) and easily enter these positions in the data processing software (Req. 2.3.1). Following a measurement, a table with all the desired output parameters is provided by the data acquisition and processing subsystem (Req. 4.9), separated per magnetometer location (Req. 4.10). Thus the measurement system meets most of its requirements, and can be used as envisioned, with some limitations being imposed by the failed requirements.

Validation
The system validation is conducted to ensure that the system fulfills the research objective. To this end, a user test case has been designed to characterize the magnetic field of Delfi-PQ. In this test, three magnetometer configurations are used. The first one investigates the effect of Delfi being in a folded versus a deployed state. The second configuration investigates the magnetic field around the battery pack and the third configuration investigates how the magnetic field varies with the vertical coordinate. All three configurations include measurements on both the passive and active magnetic field of the satellite. In addition, a longer measurement is conducted to investigate dynamic effects of Delfi-PQ.

The functional validation showed that the measurement system is capable of measuring the magnetic field produced by Delfi-PQ. The passive field is measured at all magnetometer positions in all three configurations, whereas an active field was only measured in close proximity to the battery pack. Changing between the different magnetometer configurations was done rapidly due to the modular design of the measurement system. The measurement system is capable of measuring dynamic effects, as the data transmission of the communications subsystem is seen in the measurement results.
However, the measurement system is not designed to conduct measurements on Delfi-PQ in its deployed state. Being able to conduct measurements on Delfi-PQ in its deployed state should have been amongst the requirements specified in Chapter 2. This was fixed in a quick workaround, but the resulting measurements feature a repeatability error up to 0.2 µT in the individual axes. The repeatability error in the total measured magnetic field is 0.1 µT, which is lower than the error for individual axis due to the total measured magnetic field not being dependent on orientation. The effect of this is that the measurement system can only be used to correct the error due to the satellite magnetic field on ADCS magnetometers up to an uncertainty of 0.2 µT per axis.

Thus, the measurement system can measure the passive and active field of Delfi-PQ with an uncertainty of 0.1 µT for the total magnetic field and 0.2 µT for individual axes. The system can thus be used to calibrate ADCS magnetometers with an accuracy of 0.2 µT. Different measurements can be conducted in rapid succession due to the modular design of the system. This is useful if one desires to make a scan of the DUT magnetic field, for example to identify what the most suitable location for an ADCS magnetometer is. The system can also measure dynamic effects up to the limiting frequency of 18 Hz, and can therefore be used to identify which components contribute to the dynamic part of the DUT magnetic field.

6.3. Purpose of the measurement system

The verification and validation show that the magnetic measurement system does not meet all its requirements, nor does it fulfill the research objective fully. Research question 3 reads, "What purpose can the designed magnetic measurement system fulfill, either in addition to its original purpose, or instead of its original purpose?". As the measurement system does not meet all its criteria, an investigation into what the system *can* be used for it needed. In this section, various ways in which the measurement system can be a useful tool for satellite design teams are described.
Current on board ADCS magnetometers are often placed on CubeSats and PocketQubes without measuring the satellite magnetic field. They are just placed as far away from the battery pack as possible [12]. Using the measurement system, the measurements of on board magnetometers can be corrected for the satellite magnetic field, with a remaining uncertainty of 0.2 µT per axis. For Delfi-PQ this would result in a reduction of the measurement uncertainty from 0.5 µT to 0.2 µT per magnetometer axis on the bottom of the satellite. This reduces the uncertainty in the magnetic inclination from 0.6 to 0.3 degrees and the uncertainty in magnetic declination from 1.5 to 0.7 degrees. These numbers only account for uncertainties due to the satellite magnetic field and the EMF model.
Next to this, the measurement system can be used to identify which locations on the satellite body have the weakest magnetic field, and are thus most suitable for on board magnetometer placement.
Furthermore, the measurement system can be used to identify the positions of the largest magnetic field sources present in the satellite. This can be a valuable functionality, as these sources can then be re-positioned to minimize electromagnetic interference.
The measurement system performed well with regards to measuring the dynamic aspects of the satellite magnetic field, up to the limiting frequency of 18 Hz. It can be used to identify frequencies which contribute to the magnetic field. This information can in turn be used to investigate which components contribute to the magnetic field.

This concludes the answers to the research questions. The measurement system does not meet all the requirements, mainly due to its measurement uncertainty of 0.2 µT per axis. Yet, it does provide a significant improvement with regards to *on board* magnetometer calibration, in addition to having other useful functions for CubeSat or PocketQube design teams. In the next section some recommendations for future work are suggested, which enable the measurement system to fulfill its original purpose and meet all the requirements.

6.4. Recommendations

In this section, recommendations for future work are discussed. These will be changes that can be made to improve the performance magnetic measurement system with regards to the requirements or fulfilling its original purpose.

- The uncertainty in the measurement system is 0.1 μT. This uncertainty is quite high, and largely present due to the measurement system being designed for a PocketQube in folded state. If the PocketQube is deployed, the system needs to be lifted between the background measurement and the measurement with the satellite present, which causes a slight difference in orientation. This can be corrected for by designing an alternative supporting structure. This new supporting structure should either void the need to be lifted, or be easier to place in the exact same location and orientation.
  The effect of this new supporting structure will likely be a lower repeatability error. Background measurements lasting 20 s where the measurement system remains in place show a standard deviation of the mean of 4 nT. So, in theory the repeatability error can fall below the required 34 nT (Req. 3.2). Next to this, a new supporting structure will yield a lower repeatability error in the x-, y-, and z-direction, as the magnetometer orientation will no longer change between measurements. This allows for further reduction in the pointing error of an ADCS magnetometer. The current pointing error, 0.3° and 0.7° for the inclination and declination respectively, can be reduced to a theoretical minimum of 0.2° and 0.3° respectively. The reduction in pointing error is limited by the uncertainty in the EMF model. The effort required for redesigning the supporting structure is not expected to be high, but 3D printing the entire structure, including a few prototypes, will take a considerable amount of time.

- The linearity error in the magnetometers has been corrected for using 2 measurement series. This is not a robust data set, which resulted in a residual linearity error averaging 0.8%. Repeating the magnetometer error with a larger data set is expected to reduce the residual linearity error.
  A better Helmholtz coil system is recommended for the calibration procedure. As the current Helmholtz coil system had a different number of turns in its coils and likely suffered from heating effects. Next to this, the current calibration procedure suffered from environmental noise, in particular from an 11.5 Hz noise source. For a repeated calibration, a noise free environment, and repeated environmental noise checks are recommended
  The effect of an improved calibration procedure will be a reduced residual linearity error, which means that the measurement system can measure larger DUT magnetic fields within the required uncertainty margin (excluding the repeatability error). If the improved calibration and previously mentioned alternative supporting structure recommendations are implemented successfully, the measurement system would fulfill its original purpose, and meet the research objective. The effort to repeat the calibration procedure is not large, provided one has a better Helmholtz coil system at hand. It is not recommended to improve on the calibration if the repeatability error has not been accounted for yet, as the repeatability error dominates over the residual linearity error.

- Requirement 3.5, regarding the measurement frequency, is currently not met. This can be solved rather easily by changing the magnetometer settings and favouring frequency over resolution. Which of these two parameters is favoured depends on the user, but for the current state of the system, favouring *frequency* is recommended. By changing the cycle count from 50 to 200, the maximum frequency can be increased from 47 Hz to 178 Hz. This comes at the expense of the resolution, which increases from 13 nT to 50 nT. This resolution increase is currently overshadowed by the repeatability error, and a higher frequency is thus recommended.

- Requirement 2.2.1, regarding the magnetometer moving range, is currently not met. This means that the magnetometers can only move over a horizontal range of 70 mm, instead of 91.6 mm. Also, the magnetometers cannot individually be moved in small increments in the vertical direction, only as a group. It is not expected that this has a large impact on the performance of the measurement system, as one could conduct separate magnetometer measurements to tackle the problem in the vertical direction, and exclude one horizontal wall to tackle the problem in the horizontal problem.
  To solve the problem in the horizontal direction, the walls need to be extended by 21.6 mm. This requires little effort, but a lot of 3D printing time. It is recommended to include this change when addressing the repeatability error mentioned previously, as this saves a lot of 3D printing time.

To solve the problem in the vertical direction, a method to move the individual magnetometers in the vertical direction is needed. A suggestion for this is to design the magnetometer holders such that they incorporate a small rails in the vertical direction.
The effect of this change would be small, as it allows for very specific magnetometer placement which can also be achieved by doing separate measurements. For measurements with the purpose of measuring dynamic effects this change does extend the range of magnetometer configurations greatly, yet this is only relevant when one desires a specific magnetometer configuration which would be enabled by implementing this change. The effort to redesign not only the magnetometer holders, but also the rest of the supporting structure to facilitate this is expected to be large. In view of how the system has currently been used, it is not recommended to pursue this improvement unless one is absolutely sure that it is worth the effort.

The first two recommendations are the most relevant, as implementing them successfully results in the research objective being met.

A

Appendix A, 3D drawings of the supporting structure

3D drawings of all the components of the measurement system, all units in mm.

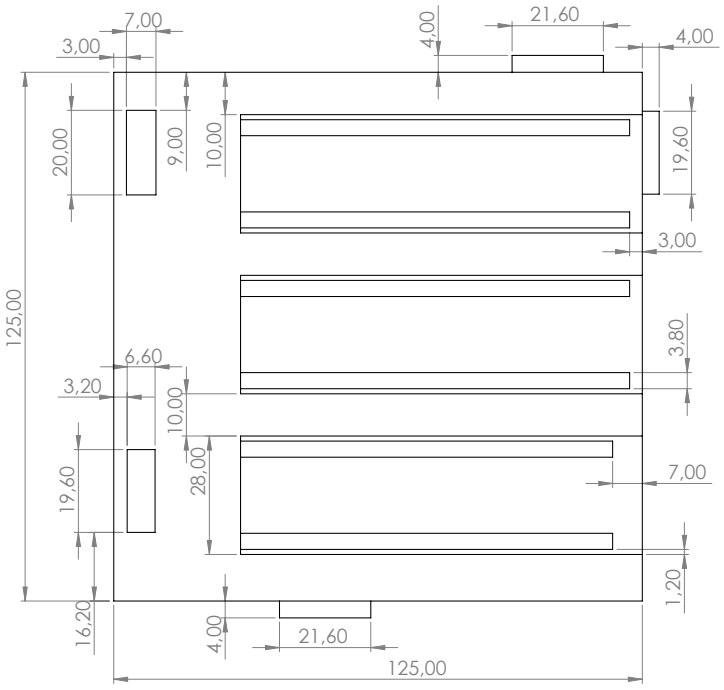

Figure A.1: Side wall 3D drawing, front view.

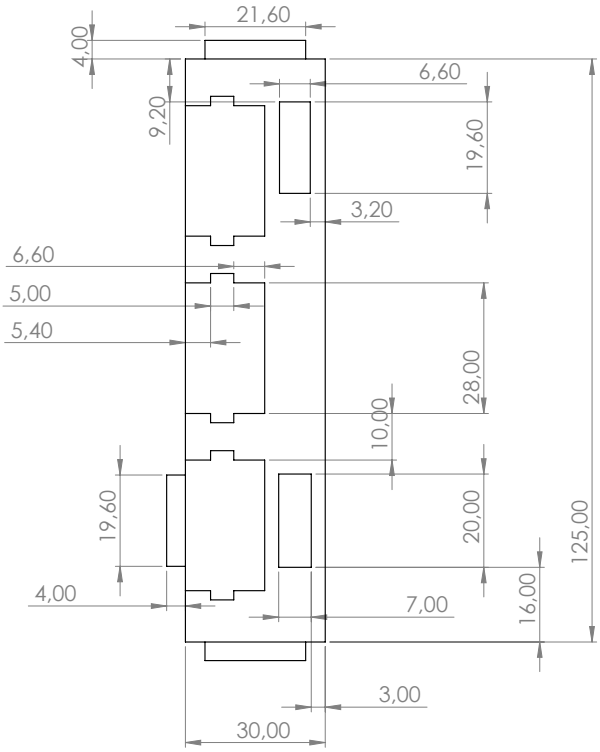

Figure A.2: Side wall 3D drawing, side view.

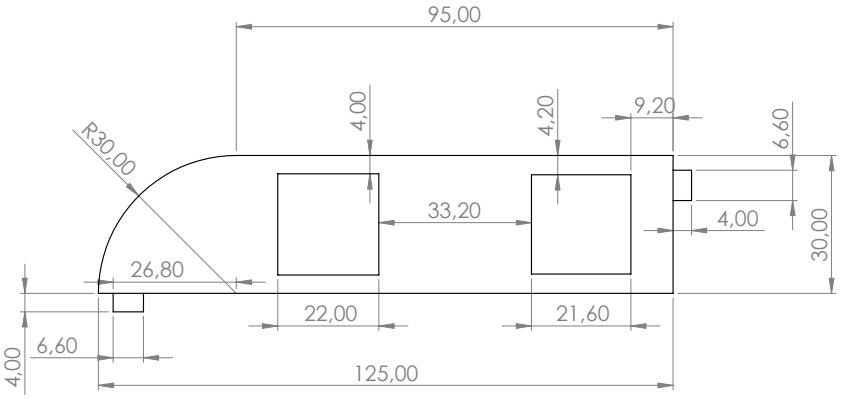

Figure A.3: Side wall 3D drawing, top view.

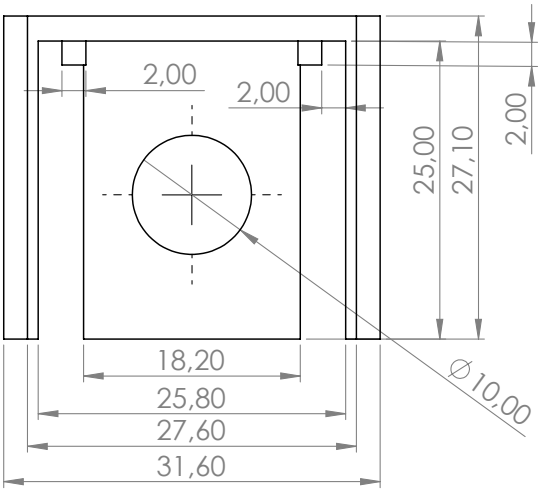

Figure A.4: Magnetometer holder main body, top view. Indent of 2 mm not visible.

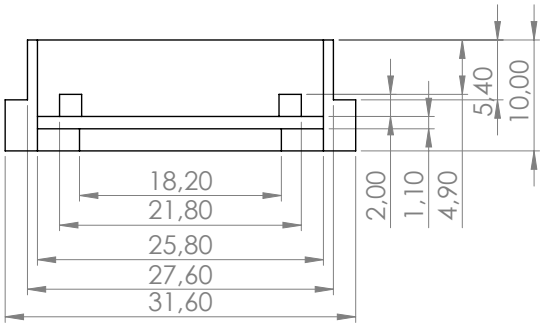

Figure A.5: Magnetometer holder main body, front view. Dimension of 2 mm indent not visible.

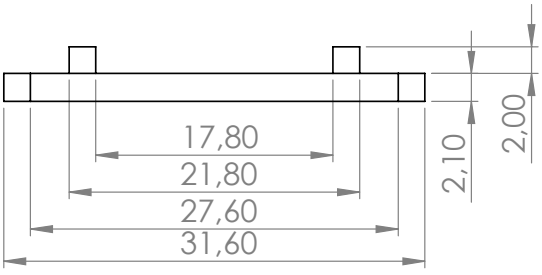

Figure A.6: Magnetometer holder side plate, top view. Indent of 2 mm not visible.

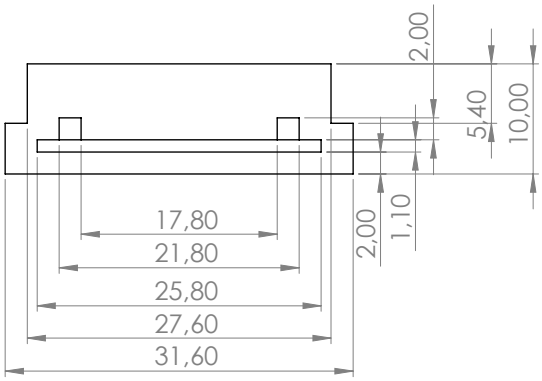

Figure A.7: Magnetometer holder side plate, front view. Dimension of 2 mm indent not visible.

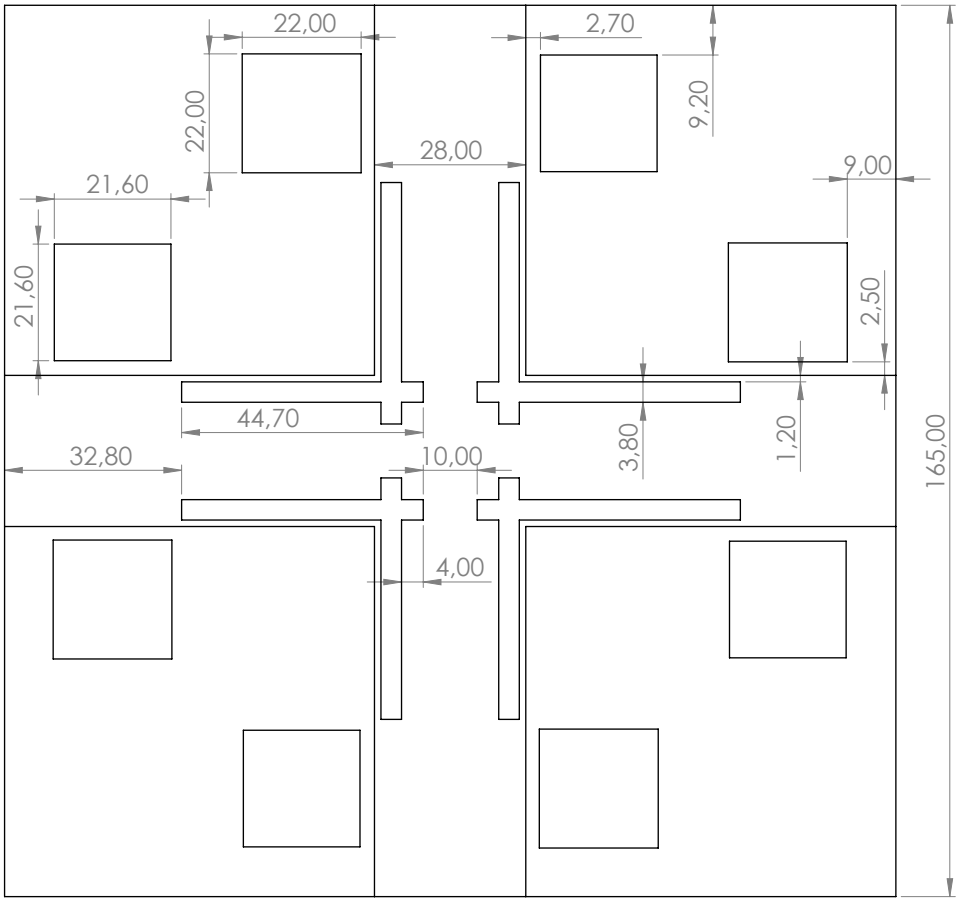

Figure A.8: Bottom/top plate 3D drawing, top view.

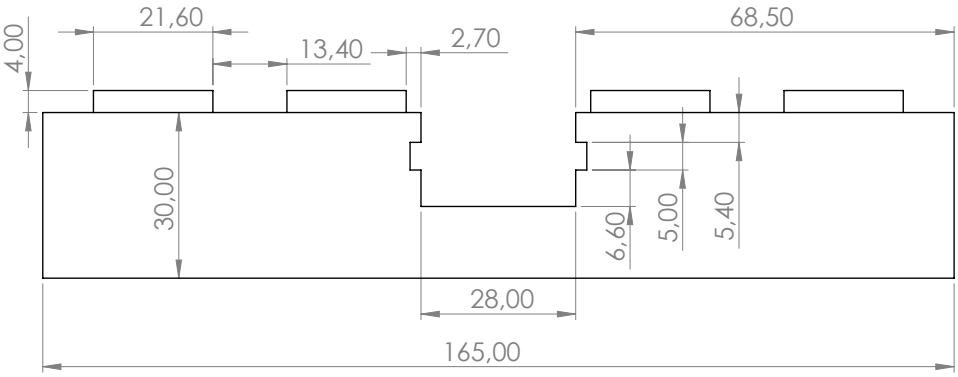

Figure A.9: Bottom/top plate 3D drawing, side view.

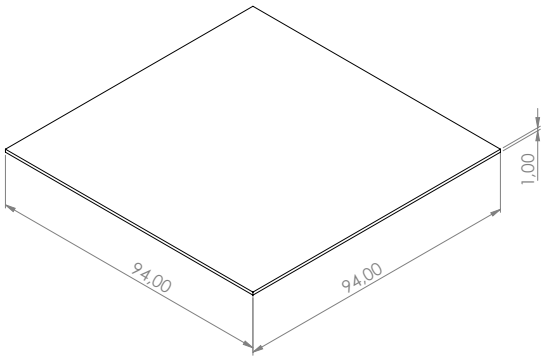

Figure A.10: Thin plate 3D drawing.

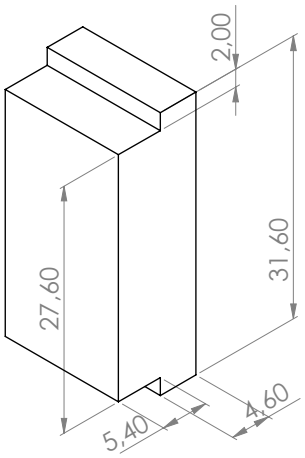

Figure A.11: Distance holder 3D drawing.

B

Appendix B, User manual

In this appendix the user manual for the measurement system is presented. To use the measurement system, the user will need the following items;

- The measurement system, stored in a box in the TU Delft AeroSpace cleanroom on floor 8.
- A laptop with Arduino IDE (not the Windows store version) and Matlab R2021b (or a later version).
- The zip file with the Arduino and Matlab scripts. The zip file can be requested from dr. ir. Jasper Bouwmeester.
- The zip file with the 3D drawings, if the user desires to redesign one or multiple components. The zip file can be requested from dr. ir. Jasper Bouwmeester.

B.1. Physical components

In the box the user will find the 3D printed components which form the supporting structure. The user needs to decide on a magnetometer configuration, and place the magnetometer holders, horizontal walls, bottom and top plate in place. After doing so, the wires which are to be connected to the magnetometers can be led through the wire slits in the walls, and be connected to the magnetometers. These can in turn be placed in their holders. The magnetometer holders consist of two parts, the main body and a side plate. Place the magnetometer in the main body first, before adding the side plate. Distance holders of 14.6 mm and 50 mm are provided, if the user desires a different distance holder this needs to be 3D printed. Most rails are found to slide well, but some can be a bit coarse. This is easily solved using a file.
The wires from the magnetometers are then connected to a breadboard, which is in turn connected to the Raspberry Pi Pico, as shown in Figure B.1. The Raspberry Pi is connected to the laptop using the USB cable provided. The connections shown in Figure B.1 are repetitive, save the separate DRDY and addressing (SA0 and SA1) pins. The required connections for these pins for a four magnetometer setup can be found in Table B.1.
If the user desires to use less magnetometers they can simply be disconnected. If one desires to use more magnetometers than 4, an additional Raspberry Pi Pico is recommended.

Magnetometer	**DRDY pin**	**DRDY slot Raspberry**	**SA0**	**SA1**	**Adress**
1	1	GP13	low	low	0x20
2	2	GP12	high	low	0x21
3	3	GP9	low	high	0x22
4	4	GP8	high	high	0x23

Table B.1: Magnetometer connections and addresses.

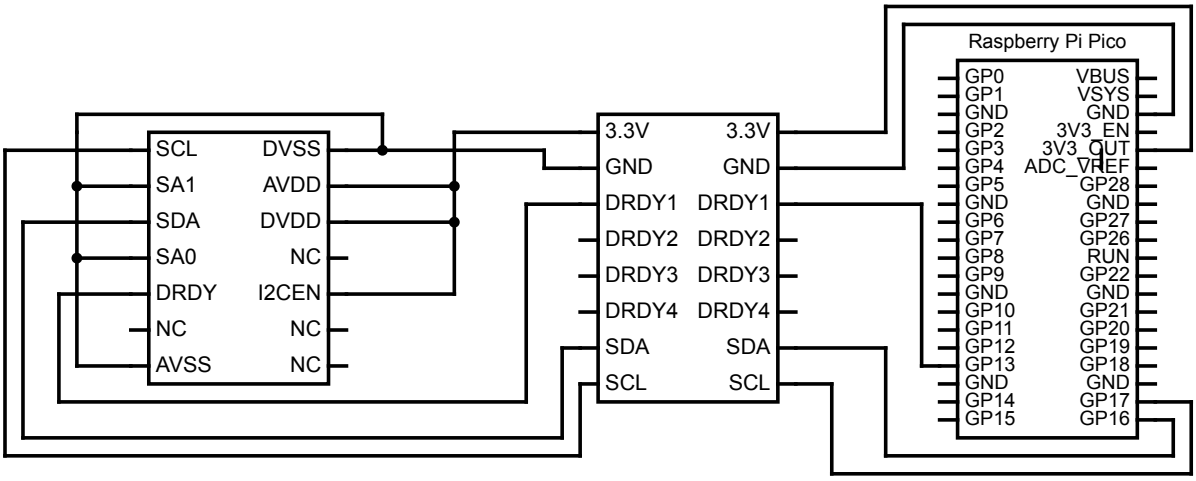

Figure B.1: The circuit used for the data acquisition. The magnetometer, breadboard and Raspberry Pi Pico are shown from left to right.

B.2. Software

The software needed to conduct measurements can be found in the zip file. For a basic measurement, 3 scripts are needed;

- Data_acq_4sensors (Arduino)
- Data_reader_4sensors (Matlab)
- Data_proc_4sensors (Matlab).

The user starts by opening the Arduino file and selecting the right port and board. This might include adding the Raspberry Pi Pico library (https://github.com/earlephilhower/arduino-pico). After uploading the script to the Raspberry Pi, the serial monitor starts showing measurement data. The user can change the cycle count and measurement frequency in this script. The measurement frequency is changed using the TMRC register. The register values and magnetometer frequencies are shown in Figure B.2. It should be noted that increasing the TMRC register above the cycle count limiting frequency has no effect. Once the Arduino script is uploaded, the serial monitor should be closed.
To start a measurement, one opens the Matlab file "Data_reader_4sensors". The measurement frequency should also be given as an input here, in addition to the measurement duration. The right serial port needs to be selected here aswell, similar as in the Arduino script. The measurement is started by pressing run, and is saved under the name defined at the bottom of the script.
Data processing is done in the Matlab script "Data_proc_4sensors". The data processing software requires two input files from the user. One file with the measurement data, and one file with a background measurement data. The user should also input the magnetometer positions, such that they can be graphically displayed by the data processing software. Lastly, the user has to provide the calibration factors for each axis of each magnetometer, found during the calibration procedure as described in Chapter 4. The output is displayed graphically, as well as saved under the name defined at the bottom of the script.

TMRC Value (Hex)	Time Between Readings	Update Rate
92	~1.7 ms	~600 Hz
93	~3 ms	~300 Hz
94	~7 ms	~150 Hz
95	~13 ms	~75 Hz
96	~27 ms	~37 Hz
97	~55 ms	~18 Hz
98	~110 ms	~9 Hz
99	~220 ms	~4.5 Hz
9A	~440 ms	~2.3 Hz
9B	~0.8 s	~1.2 Hz
9C	~1.6 s	~0.6 Hz
9D	~3.3 s	~0.3 Hz
9E	~6.7 s	~0.015 Hz
9F	~13 s	~0.075 Hz

Figure B.2: Table with the TMRC register values for different magnetometer measurement frequencies [3].

B.3. Calibration

In Chapter 6 it is recommended to improve the calibration. If this is done, the script called "Calib_RM3100_1sensor" can be used. Calibration is done separately for each magnetometer axis. Using the holder provided in the box, the magnetometer can be mounted in the middle of a Helmholtz coil system in all three directions. A measurement is conducted for various current strenghts of the HC system using the "Data_reader_4sensors" script. The data files are given as input to the "Calib_RM3100_1sensor" script, and the current values need to be input by hand. Next to this one needs to select which direction is calibrated. The script will output the calibration factor, repeating this process yields multiple calibration factors, which can be used to decrease the residual linearity error as described in Chapter 4.

Bibliography

[1] Radu S et al. The pocketqube standard. 2018.

[2] St. Olaf college. Precision vs accuracy. 2022.

[3] *RM3100 RM2100 Sensor Suite User Manual*, 2022.

[4] Andrew Leuzinger and Andrew Taylor. Magneto-inductive technology overview. *PNI white paper*, 2010.

[5] David J Griffiths. *Introduction to electrodynamics*. Prentice Hall New Jersey, 1981.

[6] NM Suhadis. Statistical overview of cubesat mission. In *Proceedings of International Conference of Aerospace and Mechanical Engineering 2019*, pages 563–573. Springer, 2020.

[7] NM Suhadis. Statistical overview of cubesat mission. In *Proceedings of International Conference of Aerospace and Mechanical Engineering 2019: AeroMech 2019, 20–21 November 2019, Universiti Sains Malaysia, Malaysia*, pages 563–573. Springer, 2020.

[8] Michael Swartwout. The first one hundred cubesats: A statistical look. *Journal of small Satellites*, 2(2):213–233, 2013.

[9] Jeffery T King, Jonathan Kolbeck, Jin S Kang, Michael Sanders, and Michael Keidar. Performance analysis of nano-sat scale μcat electric propulsion for 3u cubesat attitude control. *Acta Astronautica*, 178:722–732, 2021.

[10] Jian Guo, Jasper Bouwmeester, and Eberhard Gill. In-orbit results of delfi-n3xt: Lessons learned and move forward. *Acta Astronautica*, 121:39–50, 2016.

[11] Xiwang Xia, Guowen Sun, Keke Zhang, Shufan Wu, Tian Wang, Lei Xia, and Shanwu Liu. Nanosats/cubesats adcs survey. In *2017 29th Chinese Control And Decision Conference (CCDC)*, pages 5151–5158. IEEE, 2017.

[12] Tim Neilsen, Cameron Weston, Chad Fish, and Bryan Bingham. Dice: Challenges of spinning cubesats. In *37th Annual AAS Guidance and Control Conference, Breckenridge, CO*, 2014.

[13] L Trougnou. Ecss space systems electromagnetic compatibility handbook. In *2012 ESA Workshop on Aerospace EMC*, pages 1–6. IEEE, 2012.

[14] Anargyros T Baklezos, Christos D Nikolopoulos, Sotirios T Spantideas, Elpida G Chatzineofytou, Marco Nicoletto, Ilario Marziali, Demis Boschetti, and Christos N Capsalis. Steady state emissions modeling of low frequency magnetic and electric fields generated by goce cdmu. In *2019 ESA Workshop on Aerospace EMC (Aerospace EMC)*, pages 1–5. IEEE, 2019.

[15] H Kügler. Performance improvement of the magnetic field simulation facility mfsa. In *Environmental Testing for Space Programmes*, volume 558, pages 407–414, 2004.

[16] A Junge and F Marliani. Verification of dc magnetic model predicitions at spacecraft level. In *2012 ESA Workshop on Aerospace EMC*, pages 1–4. IEEE, 2012.

[17] George Ellwood Dieter, Linda C Schmidt, et al. *Engineering design*, volume 4. McGraw-Hill Higher Education Boston, 2009.

[18] Yousef Haik, Sangarappillai Sivaloganathan, and Tamer M Shahin. *Engineering design process*. Cengage Learning, 2015.

[19] Crispin Hales and Shayne Gooch. *Managing engineering design*. Springer, 2004.

[20] Elena Rodríguez-Rojo, Javier Cubas, and Santiago Pindado. On the upmsat-2 attitude determination and control subsystem's magnetometers integration. In *Journal of Physics: Conference Series*, volume 2090, page 012099. IOP Publishing, 2021.

[21] Nobuo Sugimura, Toshinori Kuwahara, and Kazuya Yoshida. Attitude determination and control system for nadir pointing using magnetorquer and magnetometer. In *2016 IEEE Aerospace Conference*, pages 1–12. IEEE, 2016.

[22] Halil Ersin Soken. A survey of calibration algorithms for small satellite magnetometers. *Measurement*, 122:417–423, 2018.

[23] John C Springmann and James W Cutler. Attitude-independent magnetometer calibration with time-varying bias. *Journal of Guidance, Control, and Dynamics*, 35(4):1080–1088, 2012.

[24] William J Brown, Ciarán D Beggan, Grace A Cox, and Susan Macmillan. The bgs candidate models for igrf-13 with a retrospective analysis of igrf-12 secular variation forecasts. *Earth, Planets and Space*, 73(1):1–21, 2021.

[25] Arnaud Chulliat, William Brown, Patrick Alken, Ciaran Beggan, Manoj Nair, Grace Cox, Adam Woods, Susan Macmillan, Brian Meyer, and Michael Paniccia. The us/uk world magnetic model for 2020-2025. 2020.

[26] Matthew R Walker and Andrew Jackson. Robust modelling of the earth's magnetic field. *Geophysical Journal International*, 143(3):799–808, 2000.

[27] Honeywell. *Magnetoresistive Sensor ICs V.01*, 2015.

[28] Honeywell. *Magnetoresistive Position Sensors, SS552MT Surface Mount Sensor V.01*, 2003.

[29] Liam Swanepoel, Nouf Alsharif, Alexander Przybysz, Pieter Fourie, Pierre Goussard, Mohammad Asadullah Khan, Abdullah Almansouri, and Jurgen Kosel. A facile magnetic system for tracking of medical devices. *Advanced Materials Technologies*, 6(6):2100346, 2021.

[30] Xsens. *MTi-1 V.01*, 2021.

[31] Invensense. *ICM-20948 V.1.3*, 2017.

[32] Toshiba. *TOSHIBA CMOS Digital Integrated Circuit Silicon Monolithic V.01*, 2015.

[33] AlpsAlpine. *DATA SHEET HGDEPT021B Rev.00*, 2019.

[34] Memsic. *±16 Gauss, Ultra Small, Low Noise 3-axis Magnetic Sensor MMC3416xPJ Rev C*, 2013.

[35] Bosch. *BMM150 Geomagnetic Sensor Rev 1.4*, 2020.

[36] STMicroelectronics. *LIS2MDL Digital output magnetic sensor: ultra-low-power, high-performance 3-axis magnetometer Rev 5*, 2018.

[37] AKM. *AK09973D 3D magnetic smart switch sensor V.0*, 2020.

[38] Infineon. *TLE493D-W2B6 Low Power 3D Hall Sensor with I2C Interface and Wake Up Function Ver 1.2*, 2019.

[39] Infineon. *TLE493D-A2B6 Low Power 3D Hall Sensor with I2C Interface Ver 1.3*, 2019.

[40] Memsic. *±30 Gauss, Monolithic, High Performance, Low Cost 3-axis Magnetic Sensor MMC5603NJ Rev. B*, 2018.

[41] Infineon. *TLV493D-A2BW Low power 3D Hall sensor with I2C interface 1.0*, 2021.

[42] Memsic. *±30 Gauss, Monolithic, High Performance, Low Cost 3-axis Magnetic Sensor MMC5603NJ Rev. B*, 2018.

[43] Allegro Microsystems. *ALS31313 Automotive Grade, 3D Linear Hall-Effect Sensor with I2C Output and Advanced Low Power Management Rev 9*, 2021.

[44] AKM. *AK09915 3-axis Electronic Compass V 02*, 2016.

[45] AKM. *AK09918 3-axis Electronic Compass V 00*, 2016.

[46] Melexis. *MLX90393 Datasheet Rev 008*, 2022.

[47] Infineon. *TLE493D-P2B6 High Accuracy Low Power 3D Hall Sensor with I2C Interface V 01*, 2021.

[48] Memsic. *±30 Gauss, Monolithic, High Performance, Low Cost 3-axis Magnetic Sensor MMC3630KJ Rev. A*, 2016.

[49] Texas Instruments. *TMAG5273 Low-Power Linear 3D Hall-Effect Sensor With I2C Interface Rev A*, 2021.

[50] Melexis. *MLX90363 Magnetometer IC with High Speed Serial Interface Rev 006*, 2016.

[51] Texas Instruments. *TMAG5273 Low-Power Linear 3D Hall-Effect Sensor With I2C Interface Rev A*, 2021.

[52] Melexis. *MLX90395 Triaxis® Magnetometer Node Rev 06*, 2020.

[53] Honeywell. *Three-axis Compass with Algorithms HMC6343 V 1*, 2014.

[54] Murata. *Magnetic Switch MRMS205A Data Sheet.*

[55] Pletronics. *SM45-18 Datasheet V 01*, 2009.

[56] Murata. *MRSS29DR-001 Datasheet Ver 10.*

[57] Melexis. *MLX90397 3D Magnetometer Datasheet Rev 001*, 2228.

[58] Memsic. *±8 Gauss, High Performance 3-axis Magnetic Sensor MMC5983MA Rev A*, 2019.

[59] PNI Sensor Corp. *User Manual RM3100 RM2100 Sensor Suite R09*, 2022.

[60] Leonardo H Regoli, Mark B Moldwin, Connor Raines, Tom A Nordheim, Cameron A Miller, Martin Carts, and Sara A Pozzi. Radiation tolerance of the pni rm3100 magnetometer for a europa lander mission. *Geoscientific Instrumentation, Methods and Data Systems*, 9(2):499–507, 2020.